Chapter One

1.1 Introduction

Liver diseases are considered seriously because of the liver's vital importance to human beings. Several distinct types of tumors can develop in the liver because the liver is made up of various cell types. These tumors can be benign or malignant (cancerous). The benign tumors of the liver seen most frequently include cavernous hemangioma , liver cell adenomas, and focal nodular hyperplasia (FNH).The malignant tumors of the liver seen most frequently are hepatocellular carcinoma, intrahepatic cholangiocarcinoma, Bile duct cystadenocarcinoma, and hepatoblastoma (Dushyant et al 2004).

Hepatocellular carcinoma (HCC) is the third leading cause of cancer related death in the world, with annual deaths of more than 500,000 worldwide (Parkin et al 2002) , the highest incidence rates being in eastern and southeastern Asia, sub-Saharan Africa, and Melanesia (Parkin 2001) The major risk factors for HCC are chronic viral hepatitis infection by hepatitis B or C virus, alcohol abuse, environmental poisoning, and genetic alteration, *etc*. The prognosis for HCC patients is still poor, mostly due to the failure of early diagnosis of the disease in symptom-free patients. (Chen 2004) . Diagnostic confirmation and assessment of disease extent are crucial for proper management of patients with hepatocellular carcinoma (HCC), and imaging studies play a crucial role in the diagnosis and staging of the disease. Currently, improvements in imaging technology make a noninvasive and reliable diagnostic assessment of hepatocellular nodules possible in the cirrhotic liver. (Byung et al 2010)

Current technologies provide a wide range of possibilities for liver imaging, which is very important for the diagnosis and staging of this tumor. The most reliable diagnostic tests are

triple-phase helical CT and triple-phase dynamic contrast enhanced magnetic resonance imaging (MRI), (Choi et al 2001)(Arguedas et al 2003) whereas hepatic angiography has fallen out of favor in most practice settings. HCC derives its blood supply predominantly from the hepatic artery, whereas the remainder of the non tumorous liver receives both arterial and portal blood. The hallmark of HCC during CT scan or MRI is the presence of arterial enhancement followed by delayed hypointensity of the tumor in the portal venous and delayed phases, ie, washout (Marrero et al 2005) . Biopsy is infrequently required prior to treatment, and the diagnosis of HCC is strongly dependent on hemodynamic features (arterial hypervascularity and washout in the venous phase) on dynamic imaging. Accurate staging of HCC is important in determining prognosis and in deciding optimal treatment for each patient. In addition, although there is a strong demand for an accurate diagnostic tool to detect smaller tumors, until now, the major challenge for radiologists in imaging cirrhosis is the characterization of small hepatocellular nodules in the cirrhotic liver(Byung et al 2010) .

Many image processing techniques have been developed over the past two decades to help radiologists in detection of diseases. Today several techniques are used for imaging such as Computerized Tomography (CT) and Magnetic Resonance Imaging (MRI scan). Nevertheless, these techniques can detect the disease only in its advanced stages, which leads to the death of a number of the patients. Hence, we need techniques to diagnose in its early stages (Chii-Jen & You-Wei 2012). On the other hand, there are several limitations to the assessment of HCC using only the vascular criteria. The enhancement pattern of small HCC depends on size and cellular differentiation and HCCs smaller than 2 cm may have atypical enhancement. Moreover, the diagnosis of HCC based on vascular pattern may overlook the hypovascular tumors. Conversely,

52% of small early arterial-enhancing lesions decrease in time and can be considered pseudolesions (Shimizu et al 2003) .

Computed Tomography (CT) in now a widely applied tool for diagnosis of hepatic tumors. The visual analysis of image series, acquired usually before a contrast injection and during its propagation, enables doctors to detect lesions and to recognize, to a certain extent, the type of pathology. However, in most cases, visual inspection of CT scans could not be sufficient for proper image interpretation. Even for experienced radiologists, the correct differentiation of tumor affected tissue is a difficult task. The definitive diagnosis often requires invasive procedures like needle biopsy or even surgery, which carry a risk of complications (Bruno et al 1997). CT findings are often not specific and can change during the course of the disease. In addition, the CT changes often have more than one pathological correlate, However the interpretation and diagnosis of the CT image could be varies from specialist to another one, based on their experience, degree of the vision, and the spatial resolution of the system and in turn will affect the final intended prognosis. The above variation of the parameters that affecting the final diagnosis could be overcome by utilizing mathematical digitalization and pixilation of the analog images. hence the diagnosis will be rely on the qualitative interpretation.

Computerized methods, which extract information from medical images, are being widely studied nowadays in order to replace the old methods through a new, non-invasive technology . Texture is a fundamental visual property which is essential especially in tissue characterization and in pathological structures recognition. Texture-based methods are implemented in association with classifiers in order to perform automatic tumor differentiation for various kinds of organs(Yoshida, et al 2003, Chikui, et al 2003, Madabhushi et al 2005) . The new computer-aided image processing methods (in particular methods of their texture analysis), in combination

with effective classification algorithms, can considerably improve the accuracy of the diagnosis. Extracting the information not normally detected by the human eye those techniques could reduce or even eliminate the necessity of performing the invasive techniques (Bruno et al 1997) . The texture analysis consists in extracting a set of numerical parameters (so-called texture features) to characterize Regions of Interest (ROIs) defined in the organs under study. Each of the texture parameters expresses a specified property of the texture, like coarseness, homogeneity, or the local contrast. The analysis of texture parameters is a useful way of increasing the information obtainable from medical images. So far, a great variety of texture features extraction methods has been investigated , (Galloway 1975). It is an ongoing field of research, with applications ranging from the segmentation of specific anatomical structures and the detection of lesions, to differentiation between pathological and healthy tissue in different organs. Texture analysis uses radiological images obtained in routine diagnostic practice, but involves an ensemble of mathematical computations performed with the data contained within the images. Texture features are, in fact, mathematical parameters computed from the distribution of pixels, which characterize the texture type and thus the underlying structure of the objects shown in the image. According to the methods employed to evaluate the inter-relationships of the pixels, the forms of texture analyses are categorized as structural, model-based, statistical and transform methods (Castellano et al 2003).

The use of medical imaging and tissue characterization techniques is becoming increasingly popular in diagnosis, treatment and research. However, in the case of liver disease, characterization of hepatic lesions from Computed Tomography (CT) or B-Scan Ultrasound is troublesome, even for experienced radiologists, and often requires confirmation by biopsies, or other invasive techniques, to overcome this, a variety of computer-aided diagnostic systems have

been proposed. The system involves use of different measures, such as texture features, grey scale, fractal dimension estimators or shape descriptors, combined with a classifier (Taylor P. 1998)

1.2 Problem of the study :

The correct differentiation of tumor affected liver tissue is a difficult task , Hepatocellular carcinoma (HCC) is the most frequent malignant liver tumor, it could be diagnosed by different methods, this diagnosis is just relying on visual percussion (hypothesis). Therefore a biopsy should be done for confirmation; generally it is taken by fine needle aspiration which invasive , Moreover liver has different positions and very similar intensity values with the adjacent organs that are kidney, spleen and stomach in addition to the variation of the intensity throughout the liver from the right lobe to the left lobe including the other lobes, therefore additional method should be applied to characterize and classify the HCC and the liver in the abdominal CT images .

1.3 Objectives:

1.3.1 General objective:

The main aim of this study was to characterize Hepatocellular carcinoma (HCC) in CT images using texture analysis, in order to have an objective method to improve the accuracy of the diagnosis and to reduce the number of invasive procedures .

1.3.2 Specific Objectives of the Study:

- To characterize the hepatocellular carcinoma pre and post contrast .
- To delineate the HCC outline in CT images .
- To classify the abdominal CT image into HCC, liver ,kidney and spleen.

- To find the accuracy of the applied algorithm and the classification power of the applied textural features and grey level .
- To generate outline function that can identify the HCC on CT image in routine work.

1. 4 Important of the study:

- This study will provides a means to classify the CT images which will help image interpretation by the radiologist and improve the accuracy of the diagnosis ,
- Accurately delineation the tumor, and potential areas of tumor involvement on CT images particularly apparent in radiotherapy where the aim is to deliver as high a radiation dose as possible to diseased tissue whilst limiting the radiation dose to healthy tissue.

1. 5 Overview of the study:

Chapter one was an introduction .chapter two overviewed the available literatures. Whereas chapters three demonstrated the methodology used in the study. Chapter four presented the obtained result and analysis, and finally chapter five discussed the result and states the conclusions, and recommendation, Appendix and reference.

Chapter two

Literature review

2.1 Liver Anatomy

The liver is the largest of the abdominal viscera, occupying a substantial portion of the upper abdominal cavity. It occupies most of the right hypochondrium and epigastrium, and frequently extends into the left hypochondrium as far as the left lateral line. As the body grows from infancy to adulthood the liver rapidly increases in size. This period of growth reaches a plateau around 18 years and is followed by a gradual decrease in the liver weight from middle age. The ratio of liver to body weight decreases with growth from infancy to adulthood. The liver weigh approximately 5% of the body weight in infancy and it decreases to approximately 2% in adulthood. The size of the liver also varies according to sex, age and body size. It has an overall wedge shape, which is in part determined by the form of the upper abdominal cavity into which it grows. The narrow end of the wedge lies towards the left hypochondrium, and the anterior edge points anteriorly and inferiorly. The superior and right lateral aspects are shaped by the anterolateral abdominal and chest wall as well as the diaphragm. The inferior aspect is shaped by the adjacent viscera. The capsule is no longer thought to play an important part in maintaining the integrity of the shape of the liver. Throughout life the liver is reddish brown in colour, although this can vary depending upon the fat content. Obesity is the most common cause of excess fat in the liver (also known as steatosis) the liver assumes a more yellowish tinge as its fat content increases. The texture is usually soft to firm, although it depends partly on the volume of blood the liver contains and the fat content (Standring 2008).

2.1.1 Peritoneal attachments

The peritoneum connects the liver in 4 locations: the coronary ligament, the left and right triangular ligaments, and the falciform ligament. These connections are not true ligaments in the anatomical sense, rather they are condensed regions of peritoneal membrane that support the liver (Figure 2-1) . The wide coronary ligament connects the central superior portion of the liver to the diaphragm, the left and right triangular ligaments located on the lateral borders of the left and right lobes, respectively and connect the superior ends of the liver to the diaphragm while the falciform ligament runs inferiorly from the diaphragm across the anterior edge of the liver to its inferior border. At the inferior end of the liver, the falciform ligament forms the round ligament (ligamentum teres) of the liver and connects the liver to the umbilicus (Saladin 2009).

2.1.2 Gross Anatomical Lobes

Historically, the liver has been considered to be divided into right, left, caudate and quadrate lobes by the surface peritoneal and ligamentous attachments. Figure 2-2

2.1.2.1 Right lobe

The right lobe is the largest in volume and contributes to all surfaces of the liver. It is divided from the left lobe by the falciform ligament superiorly and the ligamentum venosum inferiorly. there are two prominences separated by the porta hepatis: the caudate lobe lies posterior, and the quadrate lobe anterior, to the porta hepatis.

2.1.2.2 Left lobe

The left lobe is the smaller of the two main lobes, although it is nearly as large as the right lobe in young children. It lies to the left of the falciform ligament with no subdivisions, and is

substantially thinner than the right lobe, having a thin apex that points into the left upper quadrant.

2.1.2.3 Quadrate lobe

The quadrate lobe is visible as a prominence on the inferior surface of the liver, It lies anterior to the porta hepatis and is bounded by the gallbladder fossa to the right.

2.1.2.4 Caudate lobe

The caudate lobe is visible as a prominence on the inferior and posterior surfaces to the right of the groove formed by the ligamentum venosum: it lies posterior to the porta hepatis. To its right is the groove for the inferior vena cava. In gross anatomical descriptions this lobe is said to arise from the right lobe, but it is functionally separate. (Standring 2008)

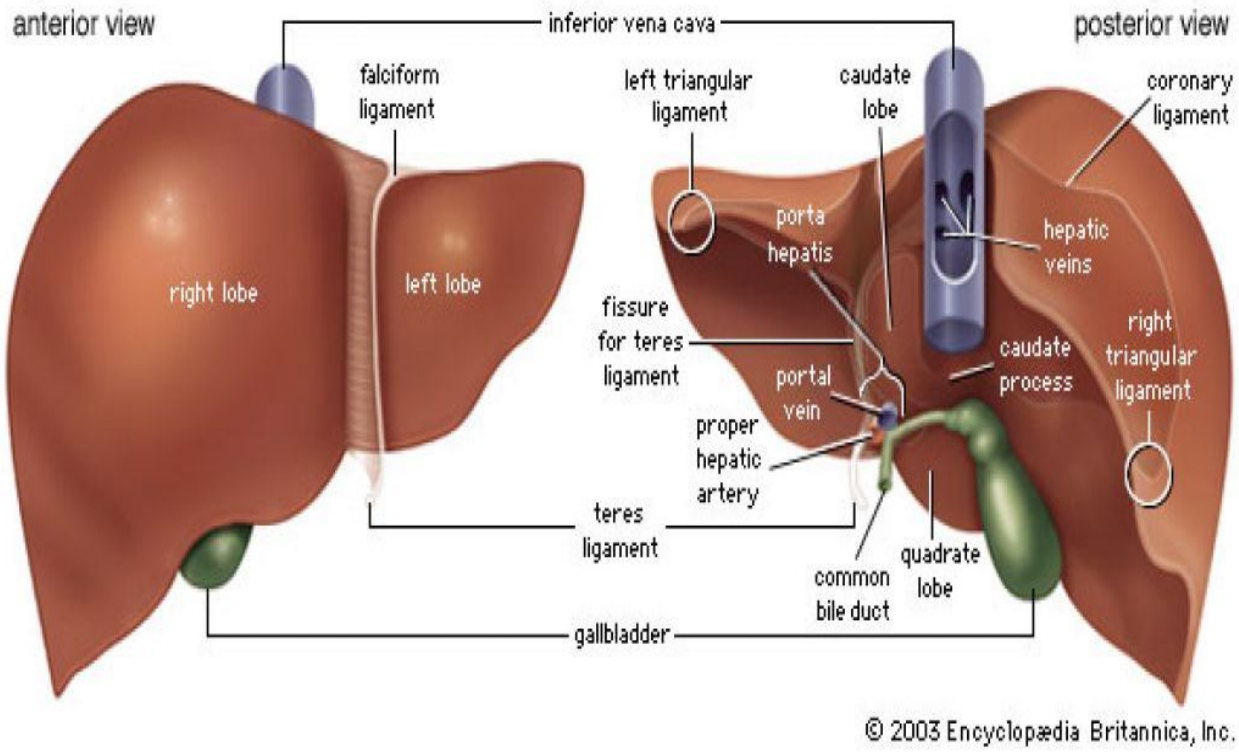

(A) **(B)**

Figure 2-1 (A and B) Anterior and posterior views of the liver: Anterior view (A) the anterior hepatic edge delineates the superior and inferior surfaces of the liver , falciform ligament divides the liver into two parts of unequal size, the right lobe and the left lobe, within the free margin of the falciform are paraumbilical veins and the round ligament ligamentum teres (Strunk, et al 2003) .

2.1.3 Segments of the Liver

The segmental terminology is now widely used. This concept is based on the description of hepatic segmentation related to the distribution of the portal pedicles and the location of the hepatic veins. According to this functional anatomy, the liver appears to be separated into two livers (hemilivers) by the main portal fissure (scissurae), also called Cantlie's line. The Cantlie's line extends from the anteroinferior gall bladder fossa posterosuperiorly to the left of the inferior vena cava. The middle hepatic vein follows this main portal fissure. These right and left hemilivers are themselves divided into two parts by two other portal scissurae. The four subdivisions are called sectors (according to Couinad's nomenclature).

The right portal scissura divides the right liver into two sectors – anteromedial or anterior and posterolateral or posterior. Along the right portal scissura runs the right hepatic vein. Each of these two sectors further divided into two segments. The anterior sector divides into segment V inferiorly (anteriorly) and segment VIII superiorly (posteriorly). The posterior sector divides into segment VI inferiorly (anteriorly) and segment VII superiorly.

The left portal scissura divides the left liver into two sectors anterior andposterior. The anterior sector is divided by the umbilical fissure into two segments -medially the segment IV, the anterior part of which is the quadrate lobe and laterallysegment III, which is the anterior part of the left lobe. The posterior sector iscomprised of only one segment, segment II, which is posterior part of the left lobe. As a result, the two hemilivers, each of them divided into two sectors, comprise seven segments. (Segments II to segment VIII).

The spigelian (caudate) lobe or segment I must be considered from the functional point of view as an autonomous segment for its vascularisation is independent of the portal division and of the three main hepatic veins. It receives vessels from the left, but also from the right branches of the

portal vein and hepaticartery. Its hepatic veins are independent and end directly into inferior vena cava. (Rutkauskas 2006)

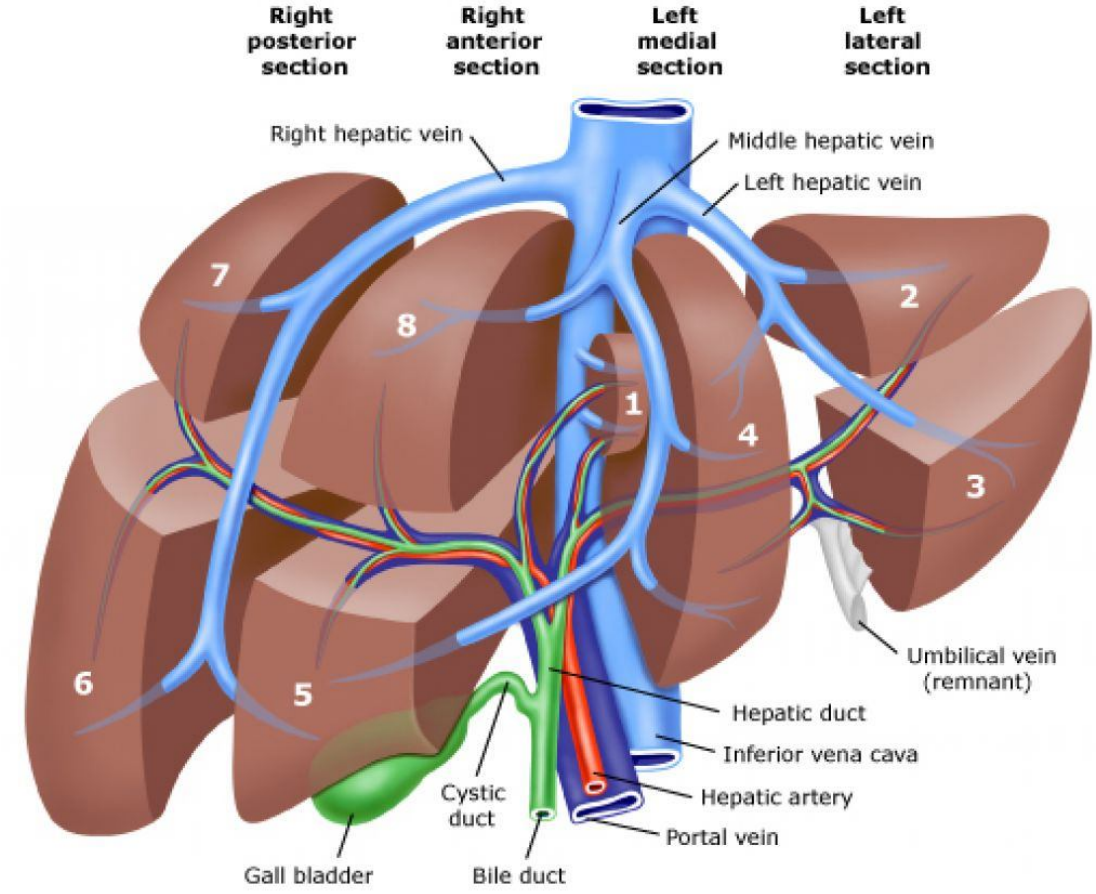

Figure 2-2 Schematic depiction of segmental liver anatomy and the normal portal venous structures. shows hepatic segments . (Rutkauskas 2006)

2.1.4 Cells of the liver

Cells of the liver include hepatocytes , about 80% of the liver volume and 60% of its cell number (parenchymal cells), hepatic stellate cells (also known as perisinusoidal lipocytes, or Ito cells), sinusoidal endothelial cells, macrophages (Kupffer cells), the cells of the biliary tree , and connective tissue cells of the capsule and portal tracts .

2.1.5 Structure of the liver

The liver is composed of numerous functional units called lobules. Within each lobule, epithelial cells called hepatocytes are arranged in layers that radiate out from a central vein. Hepatic sinusoids are spaces that lie between groups of layers, while smaller channels called bile canaliculi separate other layers. Each of (usually) six corners of the lobule are occupied by three vessels: one bile duct and two blood vessels (a portal triad). The blood vessels are branches from the hepatic artery (carrying oxygenated blood) and from the hepatic portal vein (carrying deoxygenated but nutrient-rich blood from the small intestine). Blood enters the liver through the hepatic artery and hepatic portal vein and is distributed to lobules. Blood flows into each lobule by passing through the hepatic sinusoid and collecting in the central vein. The central veins of all the lobules merge and exit the liver through the hepatic vein (not the hepatic portal vein). Within the sinusoids, phagocytes called Kupffer cells (stellate reticuloendothelial cells) destroy bacteria and break down expended red and white blood cells and other debris. Hepatocytes that border the sinusoids also screen the incoming blood. They remove various substances from the blood, including oxygen, nutrients, toxins, and waste materials. From these substances they produce bile, which they secrete into the bile canaliculi, which empty into bile ducts. Bile ducts from the various lobules merge and exit the liver as a single common hepatic duct(Phillip et al 2011) .

2.1.6 The gall-bladder

The gall-bladder lies adherent to the undersurface of the liver in the transpyloric plane at the junction of the right and quadrate lobes. The gall-bladder acts as a reservoir for bile which it concentrates. It usually contains approximately 50 mL of bile which is released
through the cystic and then common bile ducts into the duodenum in response to gall-bladder contraction induced by gut hormones. When food is in the duodenum, bile flows readily from the liver and gallbladder into the duodenum. When the duodenum is empty, a sphincter muscle (hepatopancreatic sphincter) closes the hepatopancreatic ampulla, and bile backs up and fills the gallbladder. (Omar and David 2002)

2.1.7 The biliary tree

The common hepatic duct is formed by the confluence of the right and left hepatic ducts in the porta hepatis. The common hepatic duct is joined by the cystic duct to form the common bile duct. This structure courses, sequentially, in the free edge of the lesser omentum, behind the first part of the duodenum and in the groove between the second part of the duodenum and the head of the pancreas. The common bile duct usually, but not always, joins with the main pancreatic duct (Ellis 2006) .

2.1.8 Vascular supply

The vessels connected with the liver are the portal vein, hepatic artery and hepatic veins**.** The portal vein and hepatic artery ascend in the lesser omentum to the porta hepatis, where each bifurcates. The hepatic bile duct and lymphatic vessels descend from the porta hepatis in the same omentum (Standring 2008) .

2.1.8.1 Hepatic portal vein Blood from the capillaries of the stomach, small intestine, colon, pancreas, and spleen flows into two large veins, the superior inferior mesenteric vein and the splenic vein, which unite to form the portal vein . The portal vein takes approximately 75% of the blood supply to the liver ,where it branches extensively and empties blood into the sinusoids, the capillaries of the liver , from the sinusoids, blood flows into hepatic veins, to the inferior vena cava and back to the right atrium. (Valerie & Scanlon 2007)

2.1.8.2 Hepatic artery: Arterial blood is supplied via the proper hepatic artery—a branch of the common hepatic artery that has its origin at the celiac trunk of the abdominal aorta. Before reaching the porta hepatis it divides into right and left hepatic arteries and from the right branch the cystic artery is usually given off. Prior to its ascent towards the porta hepatis the hepatic artery gives rise to gastroduodenal and right gastric branches. The latter passes along the lesser curve of the stomach to supply it (Standring 2008).

2.1.8.3 The hepatic veins Three major hepatic veins (right, middle and left) are of surgical importance , The hepatic veins drain directly from the upper part of the posterior surface of the liver at an oblique angle directly into the vena cava. In addition to the three major hepatic veins, there is the umbilical vein, which is single in most cases and runs beneath the falciform ligament between the middle and left hepatic veins; it empties into the terminal portion of the left hepatic vein . Hepatic venous drainage of the caudate lobe is directly into the IVC (Omar &David 2002).

2.1.9 Lymphatic Vessels of the Liver

Lymphatic Vessels of the Liver are divisible into two sets, superficial and deep that may be grouped into :-

2.1.9.1 Convex surface: The vessels from the back part of this surface reach their terminal glands by three different routes; the vessels of the middle set, pass through the vena-caval foramen in the diaphragm and end in one or two glands which are situated around the terminal part of the inferior vena cava. From the portions of the right and left lobes, the lymphatic vessels converge to form two trunks, one of which accompanies the inferior vena cava through the diaphragm, and ends in the glands around the terminal part of this vessel; the other runs downward and forward, and, turning around the anterior sharp margin of the liver, and ends in the upper hepatic glands.

2.1.9.2 Inferior surface: The vessels from this surface mostly converge to the porta hepatis, and accompany the deep lymphatics, emerging from the porta to the hepatic glands. The deep lymphatics converge to ascending and descending trunks. The ascending trunks accompany the hepatic veins and pass through the diaphragm to end in the glands around the terminal part of the inferior vena cava. The descending trunks emerge from the porta hepatis, and end in the hepatic glands (Standring 2008).

2.1.10 Innervations

The liver has a dual innervation. The parenchyma is supplied by hepatic nerves which arise from the hepatic plexus and contain sympathetic and parasympathetic (vagal) fibres. They enter the liver at the porta hepatis and most accompany the hepatic arteries and bile ducts. The capsule is supplied by some fine branches of the lower intercostal nerves, which also supply the parietal peritoneum, particularly in the area of the ‘bare area' and superior surface.

The hepatic plexus is the largest derivative of the coeliac plexus and receives branches from the anterior and posterior vagi. It accompanies the hepatic artery and portal vein and their branches

into the liver, where its fibres run close to the branches of the vessels, supplying vasomotor fibres to the hepatic vessels and biliary tree, and innervating the hepatocytes directly. Multiple fine branches from the plexus supply the common and hepatic bile ducts directly; branches to the gallbladder form a delicate cystic plexus (Standring 2008) .

2.2 Normal Liver Physiology

2.2.1Digestion

The liver plays an active role in the process of digestion through the production of *bile*. Bile is a mixture of water, bile salts, cholesterol, and the pigment bilirubin. Hepatocytes in the liver produce bile, which then passes through the bile ducts to be stored in the gallbladder. When food containing fats reaches the duodenum, the cells of the duodenum release the hormone cholecystokinin to stimulate the gallbladder to release bile. Bile travels through the bile ducts and is released into the duodenum where it emulsifies large masses of fat and turns the large clumps of fat into smaller pieces that have more surface area and are therefore easier for the body to digest.

Bilirubin present in bile is a product of the liver's digestion of worn out red blood cells. Kupffer cells in the liver catch and destroy old, worn out red blood cells and pass their components on to hepatocytes. Hepatocytes metabolize hemoglobin, the red oxygen-carrying pigment of red blood cells, into the components *heme* and *globin*. Globin protein is further broken down and used as an energy source for the body. The iron-containing heme group cannot be recycled by the body and is converted into the pigment bilirubin and added to bile to be excreted from the body. Bilirubin gives bile its distinctive greenish color. Intestinal bacteria further convert bilirubin into the brown pigment stercobilin, which gives feces their brown color (Faller 2004).

2.2.2Metabolism

The hepatocytes of the liver are tasked with many of the important metabolic jobs that support the cells of the body. Because all of the blood leaving the digestive system passes through the hepatic portal vein, the liver is responsible for metabolizing carbohydrate, lipids, and proteins into biologically useful materials.

Blood entering the liver through the hepatic portal vein is extremely rich in glucose from digested food. Hepatocytes absorb much of this glucose and store it as the macromolecule glycogen. The absorption and release of glucose by the hepatocytes helps to maintain homeostasis and protects the rest of the body from dangerous spikes and drops in the blood glucose level.

Fatty acids in the blood passing through the liver are absorbed by hepatocytes and metabolized to produce energy. Hepatocytes can also produce lipids like cholesterol, phospholipids, and lipoproteins that are used by other cells throughout the body.

Amino acids entering the liver require metabolic processing before they can be used as an energy source. Hepatocytes first remove the amine groups of the amino acids and convert them into ammonia and eventually urea. Urea is less toxic than ammonia and can be excreted in urine as a waste product of digestion (Faller 2004).

2.2.3Detoxification

As blood from the digestive organs passes through the hepatic portal circulation; the hepatocytes of the liver monitor the contents of the blood and remove many potentially toxic substances before they can reach the rest of the body. Enzymes in hepatocytes metabolize many of these toxins such as alcohol and drugs into their inactive metabolites. And in order to keep hormone

levels within homeostatic limits, the liver also metabolizes and removes from circulation hormones produced by the body's own glands (Faller 2004).

2.2.4Storage

The liver provides storage of many essential nutrients, vitamins, and minerals obtained from blood passing through the hepatic portal system. Glucose is transported into hepatocytes under the influence of the hormone insulin and stored as the polysaccharide glycogen. Hepatocytes also absorb and store fatty acids from digested triglycerides. The storage of these nutrients allows the liver to maintain the homeostasis of blood glucose (Rutkauskas 2006)

2.2.5Production

The liver is responsible for the production of several vital protein components of blood plasma: prothrombin, fibrinogen, which are coagulation factors involved in the formation of blood clots, and albumins the proteins that maintain the isotonic environment of the blood so that cells of the body do not gain or lose water in the presence of body fluids (Rutkauskas 2006)

2.2.6Immunity

The liver functions as an organ of the **immune system** through the function of the Kupffer cells that line the sinusoids ,that form part of the mononuclear phagocyte system along with macrophages in the spleen and **lymph nodes**. Kupffer cells play an important role by capturing and digesting bacteria, fungi, parasites, worn-out blood cells, and cellular debris. (Rutkauskas 2006)

2.3 Liver pathology

2.3.1.Liver cirrhosis

Cirrhosis of the liver refers to scarring of the liver which results in abnormal liver function as a consequence of chronic (long-term) liver injury ,Cirrhosis of the liver is a consequence of long-term liver injury of many types, while excess alcohol use and chronic infection with hepatitis viruses (such as hepatitis B and hepatitis C) are the most common causes of cirrhosis**,** cirrhosis can be caused by other conditions including fatty liver disease, inherited disorders, drug-induced injury, bile duct disorders and autoimmune diseases. A large portion of patients (up to 20%) do not have an identifiable cause for cirrhosis, and this is known as cryptogenic cirrhosis. Cirrhosis occurs when the normal structure of the liver is disrupted by bands of scar tissue. One of the normal functions of the liver is to filter blood returning to the heart from the digestive system. When cirrhosis is present, the presence of scar tissue causes increased resistance to blood flow through the liver this results in high pressures developing in the veins that drain into the liver, a process called portal hypertension . Since the liver performs many complex metabolic functions, there are many complications that arise from cirrhosis. (Edward bittar 2004)

2.3.2 Fatty liver disease

Fatty liver disease occurs in two major forms alcoholic and nonalcoholic. with variable amounts of liver injury, inflammation , and fibrosis. Both forms of fatty liver disease are common. Alcoholic liver disease affects approximately 1 % of the adult population and accounts for half of deaths due to cirrhosis. Nonalcoholic fatty liver disease is the most common reason for liver test abnormalities in the general population and may be present in as many as a quarter of adult people. The spectrum of fatty liver disease ranges from simple steatosis

(considered benign and non-progres-sive), to steatohepatitis (fatty liver with liver cell injury and inflammation), to progressive hepatic fibrosis and cirrhosis (Edward 2004) .

2. 3. 3 hepatic cysts

hepatic cysts are abnormal fluid-filled spaces in the hepatic parenchyma and biliary tree. they are categorized into three main types , fibrocystic diseases of the liver, cystadenomas and cystadenocarcinomas, and hydatid cysts. (Sleisenger and Fordtran's 2010)

2.3.3.1.Fibrocystic diseases of the liver

Fibrocystic diseases of the liver originate from abnormal persistence or defects in the progressive remodeling of the ductal plate during development, resulting in dilated fluid-filled spaces, including hepatic and choledochal cysts, portal fibrosis, and ductal plate malformations, the more common are :

Simple Hepatic Cysts : are thought to be congenital in origin**.** They generally are smaller than 5 cm in diameter and can number up to three . The cysts usually are asymptomatic and discovered incidentally during upper abdominal imaging. They occur more often in women than in men, and their prevalence increases with age. (Sleisenger and Fordtran's 2010)

Polycystic Liver Disease : PCLD is a rare condition in which multiple cysts form in the hepatic parenchyma; usually it comes to clinical attention in adulthood . PCLD usually presents in association with autosomal dominant polycystic kidney disease (ADPKD) but can appear as isolated polycystic liver disease**.** (Sleisenger and Fordtran's 2010)

2.3.3.2 Hydatid cysts

Hydatid cysts are caused by infestation with the parasite Echinococcusgranulosus. They common in areas of sheep and cattle farming. The hydatid cyst develops an outer layer of inflammatory

tissue and an inner germinal membrane that produces daughter cysts. Patients with hydatid cysts, similar to patients with simple cysts, are most often asymptomatic, but pain may develop as the cyst grows. Cyst rupture is the most serious complication of hydatid cysts , Rupture into the biliary tree may result in jaundice or cholangitis. Free rupture into the peritoneal cavity may cause anaphylactic shock.(Edward 2004)

2.3.4 Hepatic abscesses

Hepatic abscesses can be amebic or bacterial in origin. Entamoebahistolytica is the causative agent in amebic abscesses. Amebiasis generally only involves the intestine but can invade the mesenteric venules resulting in liver abscesses. Other routes of contamination include the portal vein and hepatic artery. Patients with intra-abdominal infections may present with liver abscesses with extension of bacteria through the portal venous system. Those patients with amebiasis can have history of diarrhea and weight loss, although some may be asymptomatic. Rarely, abscesses will rupture, and patients present with peritonitis. (Edward 4004)

2.3.5 Liver Tumors

Hepatic tumors may originate in the liver—from hepatocytes, bile duct epithelium, or mesenchymal tissue—or spread to the liver from primary tumors in remote or adjacent organs. In adults in most parts of the world, hepatic metastases are more common than primary malignant tumors of the liver, whereas in children, primary malignant tumors outnumber both metastases and benign tumors of the liver. (Sleisenger and Fordtran's 2010)

2.3.5.1.Benign tumors

Hepatocellular adenoma : Hepatocellular adenomas (or hepatic adenomas) were extremely rare before the use of oral contraceptive steroids became widespread. They are still rare in men, and the development of this tumor in women who are taking or have taken contraceptive steroids strongly implies a cause and effect relationship. (Sleisenger and Fordtran's 2010).

Cavernous hemangioma : Cavernous hemangioma is the most common benign tumor of the liver and is found in as many as 7% of autopsies. Cavernous hemangiomas affect persons of all ages, although they manifest most often in the third, fourth, and fifth decades of life. Women are predominantly affected and often present at a younger age and with larger tumors in comparison with men. Cavernous hemangiomas may increase in size with pregnancy or the administration of estrogens . The great majority of cavernous hemangiomas can safely be left untreated . (Sleisenger and Fordtran's 2010)

Infantile hemangioendothelioma :, Is the most common tumor of the liver in infants . Its importance stems from the high incidence of congestive heart failure in infants with this tumor and the resulting high mortality rate. The tumor almost invariably manifests in the first six months of life and is twice as common in girls as in boys. Hepatic hemangioendothelioma often coexists with hemangiomas in other organs, especially the skin. (Sleisenger and Fordtran's 2010).

2.3.5.2.Tumor-like hepatic lesions

Focal nodular hyperplasia : usually solitary lesion composed of nodules of benign hyperplastic hepatocytes surrounding a central stellate scar. (Sleisenger and Fordtran's 2010).

2.3.5.3 Hepatic metastases

The liver is the most frequent target for metastatic spread of tumors. Hepatic metastases occur in 40% to 50% of adult patients with extrahepatic primary malignancies . Hepatic metastases

commonly originate from primary sites in the distribution of the portal venous system, including the pancreas, stomach, and colon. Outside this distribution, tumors of the lung and breast are the most common origins of hepatic metastases. (Sleisenger and Fordtran's 2010).

2.3.5.4 Malignant Tumors :-

Hepatocellular Carcinoma*:* Among primary malignant tumors of the liver, hepatocellular carcinoma is the most common .Hepatocellular carcinoma (HCC) is a malignant tumor of the hepatocytes. It is the fifth most common cancer in men and the eighth most common in women, and it ranks fourth in annual cancer mortality rates. (Parkin D 1997) . The incidence of hepatocellular carcinoma increases progressively with advancing age in all populations, although it tends to level off in the oldest age groups and is rare in children . Patients with hepatocellular carcinoma often are unaware of its presence until the tumor has reached an advanced stage. The most common, and frequently first, symptom is right hypochondrial or epigastric pain (Bosch 1997) .

cholangiocarcinoma : Cholangiocarcinoma is a malignant neoplasm arising from the biliary duct epithelium. It often carries different names based on the particular portion of the biliary tree involved—small intrahepatic bile ducts (peripheral cholangiocarcinoma), hepatic duct bifurcation (perihilar cholangiocarcinoma, or Klatskin tumor), and extrahepatic bile ducts (bile duct carcinoma). Malignant transformation of the bile duct cells generally occurs in an environment of inflammation or cholestasis (or both), usually as a result of one of the known risk factors. Congenital and acquired abnormalities of the biliary tract that may result in bile stasis, chronic inflammation, and infection, as in biliary atresia,(Kulkarni 1977) and intrahepatic cholelithiasis, have been associated with the development of cholangiocarcinoma . Cirrhosis, particularly caused by HCV, also has been associated with cholangiocarcinoma. (Yalcin S 2004)

Hepatoblastoma : In children, hepatoblastoma is the third most common malignant tumor and the most common malignant hepatic tumor. It occurs almost exclusively in the first three years of life; boys are affected twice as often as girls. , Hepatoblastoma may occur sporadically or in association with hereditary syndromes such as familial adenomatous polyposis although Beckwith-Wiedemann syndrome, suggesting a possible role for chromosomes 5 and 11 in the genesis of the tumor. (Isaacs 2007)

Hemangiosarcoma : is the most common malignant tumor of the liver. It occurs almost exclusively in adults and is most prevalent in the sixth and seventh decades of life. Men are affected four times as often as women. In early reports, the tumor became evident approximately 20 years after the patient had been exposed to thorium dioxide. (Sleisenger and Fordtran's 2010)

Epithelioid hemangioendothelioma : is a rare tumor whose incidence is not known. Two thirds of patients were female, and the tumor occurred at all ages in adulthood. . (Sleisenger and Fordtran's 2010)

2.4 Hepatocellular Carcinoma :

Hepatocellular carcinoma is a tumor of the liver, which is responsible for over 12,000 deaths per year in the United States where the incidence of the disease is approximately 2.5 per 100,000 population. It is one of the most common malignancies in adults, and is more common in men than women (2-4:1), and blacks than whites. Worldwide, over a million deaths per year (about 10% of all deaths in the adult age range) can be attributed to hepatocellular carcinoma. The occurrence of hepatocellular carcinoma varies widely depending on geographic location. Whereas incidence in the Western world is less than two per 100,000 males, it is currently 40-60 per 100,000 in Africa and parts of the Far East. In the United States, hepatocellular carcinoma is more common in people of East Asian origin. In the future, the prevalence of hepatocellular

carcinoma may increase in the United States and parts of Europe because of the high incidence of hepatitis C. At the same time, many experts expect incidence rates to decline in the Far East due to universal immunization for hepatitis B (Gurakar 2013) .

Gross Appearance of Hepatocellular carcinoma may take one of three forms— nodular, massive, or diffusely infiltrating, the nodular variety is most common and usually coexists with cirrhosis . And the HCC is classified histologically into well-differentiated, moderately differentiated, and undifferentiated forms. (Sleisenger and Fordtran's 2010).

2.4.1 Causes and Pathogenesis of HCC

In contrast to many other malignancies, for which risk factors can only sometimes be identified, the immediate cause of hepatocellular carcinoma can usually be identified and is most commonly chronic viral hepatitis or cirrhosis. Hepatocellular carcinoma is multifactorial in cause and complex in pathogenesis. Four major causative factors have been identified (Raza 2007).

Hepatitis B Virus

Some 387 million carriers of HBV exist in the world today, and hepatocellular carcinoma will develop in as many as 25% of them . HBV accounts for up to 80% of hepatocellular carcinomas, which occur with high frequency in East Asian and African populations. (Raza 2007)

Hepatitis C Virus

Approximately 170 million people in the world today are chronically infected with HCV and are at greatly increased risk for the development of hepatocellular carcinoma in the industrialized countries, HCV infection, often in combination with alcohol abuse, is emerging as a major cause of the tumor (Raza 2007).

Cirrhosis

In all parts of the world, hepatocellular carcinoma frequently coexists with cirrhosis.80 All causative forms of cirrhosis may be complicated by tumor formation . Older age and male gender were confirmed as risk factors among patients with cirrhosis.(Ioannou et al 2007)

Aflatoxin B1

Dietary exposure to aflatoxin B1, derived from the fungi Aspergillus flavus and Aspergillus parasiticus, is an important risk factor for hepatocellular carcinoma in parts of

Africa and Asia. aflatoxin B1 and HBV interact synergistically in the pathogenesis of hepatocellular carcinoma.(Chiaramonte 1999).

2.4.2. Treatment of HCC

Important advances in the treatment of hepatocellular carcinoma have occurred since the 1980s; these advances include randomized controlled trials that support the benefits of certain treatments such as chemoembolization and the multikinase inhibitor sorafenib. Because hepatocellular carcinoma is usually a combination of two diseases—usually cirrhosis with varying degrees and the cancer itself—both factors must be taken into account when selecting treatment, and the clinician should decide which is the best initial therapy (Sleisenger and Fordtran's 2010)

Resection

Resection is the treatment option for patients with solitary tumors and very well-preserved liver function, as normal bilirubin with either hepatic venous pressure gradient ≤10 mmHg or platelet count ≥100,000.

Liver Transplantation

Liver transplantation is considered to be the treatment option for patients with single tumors less than 5 cm or ≤3 nodules ≤3 cm (Milan criteria) not suitable for resection (Josep 2012).

Local ablation

Local ablation with radiofrequency or percutaneous ethanol injection is considered the standard of care for patients with BCLC 0-A tumors not suitable for surgery (Josep 2012).

Chemoembolization and transcatheter therapies

Chemoembolization is recommended for patients with BCLC stage B, multinodular asymptomatic tumors without vascular invasion or extra-hepatic spread (Josep 2012).

2.4. 3 Diagnostic evaluation of HCC

2.4.3.1.Clinical presentation

Although the typical clinical features of hepatocellular carcinoma are well recognized (including abdominal pain and weight loss in patients with cirrhosis), more patients are now being diagnosed at an early stage, when they have no specific symptoms or signs. This trend toward earlier diagnosis is probably the result of surveillance programs in patients with chronic liver disease . In far advanced disease, patients with hepatocellular carcinoma usually present with typical symptoms and signs, and diagnosis is easy. In addition, hepatocellular carcinoma often coexists with cirrhosisand the onset of hepatocellular carcinoma is marked by a sudden unexplained change in the patient's condition . Ascites may be present when the patient is first seen or may appear with progression of the tumor,(Mazzanti 2008).

2.4.3.2. Serum Tumor Markers

Serum tumor markers generally are not diagnostic for hepatocellular carcinoma by themselves but can be used in conjunction with imaging findings to diagnose hepatocellular carcinoma.

Additionally, they may raise the suspicion for hepatocellular carcinoma and lead to more sensitive and serial imaging of the liver. Many of the substances synthesized and secreted by hepatocellular carcinoma are not biologically active. The most helpful of these markers is AFP. Alpha-Fetoprotein AFP is an α1-globulin normally present in high concentrations in fetal serum but in only minute amounts thereafter. Reappearance of high serum levels of AFP strongly suggests the presence of hepatocellular carcinoma (or hepatoblastoma). With higher levels of AFP, the confidence in the diagnosis of hepatocellular carcinoma is greater. According to the American Association for the Study of Liver Diseases (AASLD) guidelines, hepatocellular carcinoma can be diagnosed with confidence in patients with a serum AFP level higher than 200 ng/mL and a mass in the liver.(Kew 1989).

2.4.3.3.Liver biopsy

Diagnostic evaluation of hepatic lesions with liver biopsy has been practiced for over half a century.When performed at specialized centers, liver biopsy offers a safe and effective means to confirm suspicious lesions for HCC. Cytologic and histologic samples can be obtained by percutaneous fine-needle aspiration (FNA) and needle core biopsy, respectively, under US or CT guidance. Histologic appearance ranges from nearly normal-appearing hepatocytes in well differentiated tumors to the largely anaplastic multinucleate giant cells characteristic of poorly differentiated HCC. Complications associated with liver biopsy are include , serious hemorrhage .infection and potential for spread of tumor from the biopsy needle track is of great concern and fuels much of the controversy surrounding the need for liver biopsy (Huang et al 1996)

2.4.3.4 Diagnostic imaging

The diagnosis of hepatocellular carcinoma generally requires imaging evidence of a focal lesion in the liver, although. Arterial hyperenhancement, particularly seen on dynamic contrast imaging

of the liver, is observed because the blood supply of hepatocellular carcinoma comes from newly formed abnormal arteries (Willatt et al 2008) .

Ultrasonography

Ultrasonography detects most hepatocellular carcinomas but may not distinguish this tumor from other solid lesions in the liver. As with all imaging methods, the sensitivity increases with increasing size of the lesion. Dynamic contrast-enhanced Doppler ultrasonography with intra-arterial infusion of CO2 microbubbles and intravenous enhanced color Doppler ultrasonography are refinements that, by characterizing hepatic arterial and portal venous flow in tumorous nodules, facilitate the diagnosis of malignant and benign hepatic nodules. But These techniques are not often performed (Kudo 1999).

Magnetic Resonance Imaging

Dynamic MRI using gadolinium contrast agents provides another way of distinguishing hepatocellular carcinoma from normal liver tissue. The performance of MRI and the findings on multiphase contrast enhancement are similar to those described for CT. Typically, the signal intensity on T1-weighted images is low. MRI may be slightly superior overall to CT, although local expertise should dictate the choice of imaging technique (Yu 2004) .

Hepatic Angiography

Since the advent of CT and MRI, the diagnostic role of hepatic angiography has decreased. Digital subtraction angiography is helpful for recognizing small hypervascular hepatocellular carcinomas but may miss early, well differentiated hypovascular tumors. Hepatocellular carcinomas often are densely vascular, although multinodular tumors may be relatively avascular (Takayasu 1997).

Computed Tomography

CT is often the preferred method for diagnosing many different cancers, since the image allows a physician to confirm the presence of a tumor and to measure its size, precise location and the extent of the tumor's involvement with other nearby tissue. Despite the excellence of CT images has been appreciably improved during the last years **(**Gunasundari 2013).

Multiphase, also called dynamic, helical computed tomography (CT) is the imaging technique of choice for the diagnosis of hepatocellular carcinoma (Colli et al 2006) . Following rapid intravenous infusion of contrast, imaging is conducted at various time intervals corresponding to the phase of contrast enhancement. Triphasic scanning denotes hepatic imaging performed before contrast administration and during arterial and venous phases. HCC tumors derive blood flow predominantly from the hepatic artery and tend to enhance during the arterial phase or 2–40 seconds after contrast infusion. The surrounding hepatic parenchyma obtains 75–80% of its blood flow through the portal vein and is best demonstrated 50–90 seconds after infusion of contrast during the portal phase. Arterial phase enhancement can increase HCC tumor detection by 10%. HCC typically appears heterogeneous on CT, which may reflect intratumoral fibrous stranding (mosaic sign), fatty metamorphosis, necrosis, or calcifications . The presence of satellite nodules in close proximity to the lesion is often characteristic. Fibrous structures within or encapsulating the lesion strongly retain contrast and enhance readily on delayed imaging (3–10 min after infusion) (Eldad. & Adrian 2005) .

When the nodule is 1 to 2 cm, guidelines recommend a second type of dynamic imaging (magnetic resonance imaging [MRI] or contrast ultrasonography) to confirm the diagnosis of hepatocellular carcinoma, CT often finds so-called hypervascular-only lesions, which enhance in the arterial phase and become isodense to the surrounding liver in the portal-venous and delayed phases. Dynamic CT is also useful for detecting invasion into the portal or hepatic veins and

identifying the location and number of tumors; these findings are critical for planning treatment. .(Luca A et al 2007)

(A)

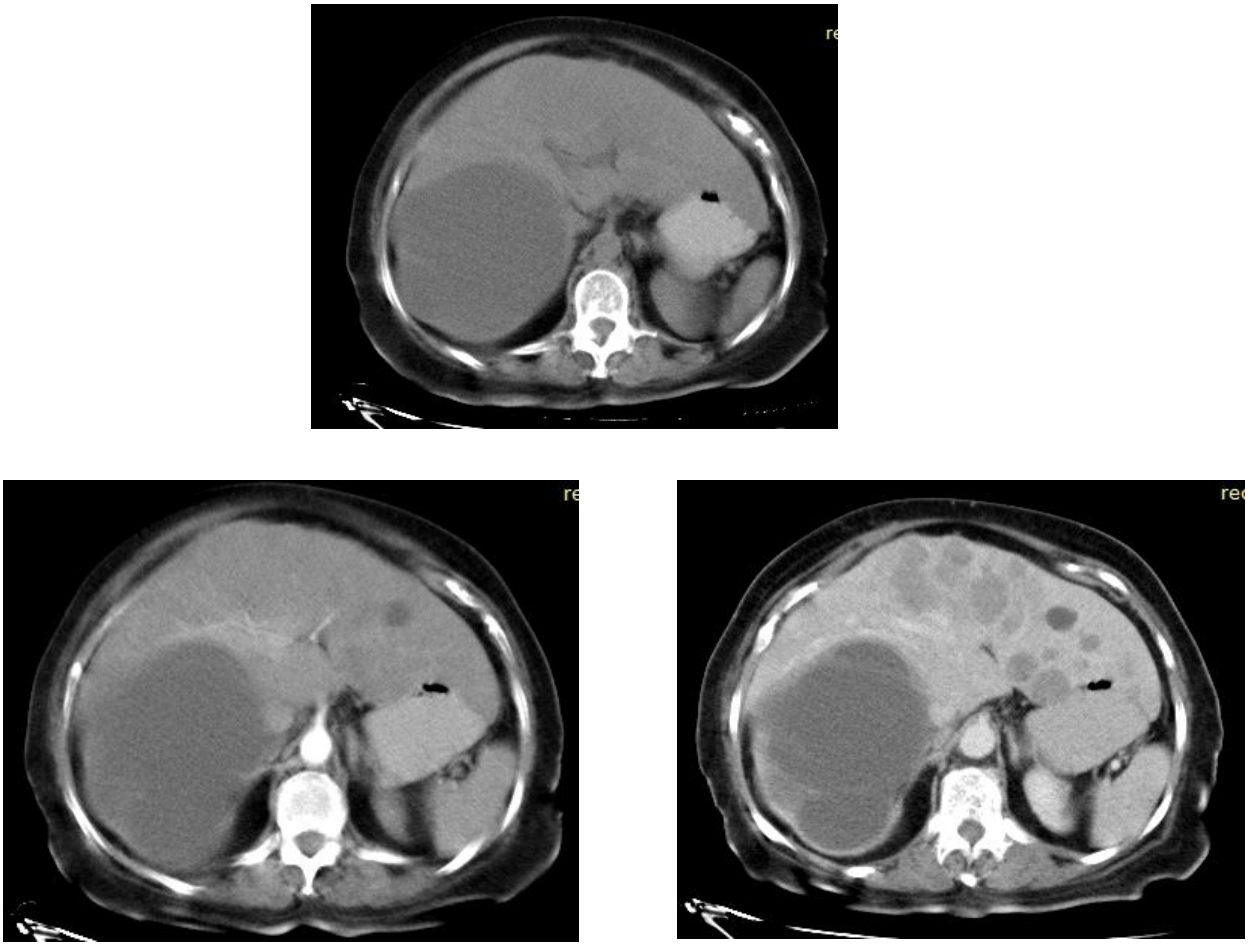

(C) (B)

Figure 2-3 Multiphase CT images Shows hepatocellular carcinoma (HCC) lesion.(A)Axial un enhanced CT scan of the liver (B) contrast-enhanced obtained during the hepatic arterial phase shows (C) Axial contrast-enhanced CT scan of the liver obtained during the hepatic venous phase at the same level as d slightly hypoattenuating (washout) compared with the surrounding liver parenchyma.

2.4.3.5 Texture analysis :

Texture analysis is an essential issue in image processing. It comprises a set of mathematical techniques used to quantify the different gray levels within an image in terms of intensity and distribution , so Image texture analysis can provide quantitative information in the form of texture features that is not visible to human vision (Heraldicet.al 1973) .Texture represents the spatial arrangement of pixels' gray levels in a region. So, it can be divided into two classes: periodic texture and random texture. Consequently, we can distinguish the structural approaches and the statistic approaches to calculate a number of mathematical parameters that characterize the texture. Structural approaches are more suited to the study of periodic or regular textures. However, statistic approaches are used to characterize fine and non homogeneous structures without apparent regularity. That is why; this type of method is generally applied in medical imaging. (Sassi1 et al 2012) A statistical approach perceives a texture as a quantitative measure of the arrangement of intensities in an area . Statistical methods can be categorized into first order (one pixel), second-order (two pixels) and higher-order (three or more pixels) . Spectral statistics, based on the number of pixels used to define the feature. (Gunasundari S 2013)

Texture is a frequently used characteristic in the analysis and understanding of images, texture analysis is presented here as a useful computational method for discriminating between pathologically different regions on medical images because it has been proven to perform better than human eyesight at discriminating certain classes of texture (Julesz, 1975) .Texture analysis methods are useful for discriminating and studying both distinct and subtle textures in multi-modality medical images. Practical implementation requires careful consideration of the power of the individual features to discriminate between textures. This is essential to reduce the influence that heavily correlated features, and features with little discriminatory power, have on

the overall classification. Statistical texture analysis techniques are constantly being refined by researchers and the range of applications is increasing (Nailon 2010). There are four major issues in texture analysis: Feature extraction to compute a characteristic of a digital image able to numerically describe its texture properties , texture discrimination to partition a textured image into regions, each corresponding to a perceptually homogeneous texture (leads to image segmentation) , texture classification to determine to which of a finite number of physically defined classes (such as normal and abnormal tissue) a homogeneous texture region belongs , shape from texture to reconstruct 3D surface geometry from texture information. (Levine 1985)

First-order histogram based features

First order statistics measures(FOS) is feature extraction techniques use the image histogram, or pixel occurrence probability, to calculate texture. The main advantage of this approach is its simplicity through the use of standard descriptors (e.g. mean and variance) to characterize the data. In general seven features commonly used to describe the properties of the image histogram, and therefore image texture, are computed. These are: mean; variance; coarseness; skewness; kurtosis; energy; and entropy. (Tuceryan & Jain 1998). The mean takes the average level of intensity of the image or texture being examined , while the variance describes the variation of intensity around the mean , the skewness is zero if the histogram is symmetrical about the mean, and is otherwise either positive or negative depending whether it has been skewed above or below the mean. Thus is an indication of symmetry , the kurtosis is a measure of flatness of the histogram and The entropy is a measure of histogram uniformity.

Information extracted from local image histograms is used in as features for texture segmentation. (Lowitz 1983)

The intensity-level histogram is a function showing (for each intensity level) the number of pixels in the whole image, which have this intensity: The histogram of intensity levels is obviously a concise and simple summary of the statistical information contained in the image. Calculation of the grey-level histogram involves single pixels. Thus the histogram contains the first-order statistical information about the image (or its fragment).

Different useful parameters (image features) can be worked out from the histogram to quantitatively describe the first-order statistical properties of the image. Most often the so-called central moments (Papoulis 1965) are derived from it to characterize the texture (Levine 1985).

2.5 previous study:

In diagnosing liver diseases, CT has become one of the major imaging modalities. Different authors have used different techniques for classification liver diseases from CT images . Comparing all methods with the help of accuracy measure.

Heng Tan et al 2011 aims to determine the quantitative method of region-of-interest (ROI) analysis of lesion attenuation on CT ,289 patients had undergone multiphasic CT scans of the liver including arterial, PV and equilibrium phases. For all cases, they recorded the CT attenuation of lesion in the all phases, as well as the corresponding CT attenuation of surrounding liver tissue in the respective phases. Qualitative assessment was performed by 2 diagnostic radiologists reading. A representative CT section containing the lesion was selected. The lesions were observed for their enhancement pattern, relative to the surrounding liver (hypodense, isodense and hyperdense) during each phase of the CT study , analyses were perform using receiver operating curves (ROC) to determine the optimal method and cut-off value for quantitative assessment of tumor wash-out. The result show that , Using a cut-off of 10 HU attenuation difference between the arterial and equilibrium phases is a simple and objective method that can be included as an adjunct to visual assessment to improve sensitivity for determining lesion wash-out on CT.

Furlan et at (2011) 30 cirrhotic patients underwent multiphasic MDCT before contrast medium administration and during hepatic arterial hepatic venous and delayed phases. Two radiologists qualitatively evaluated images for lesion attenuation. Tumor washout was evaluated subjectively and objectively. Tumor-to-liver contrast (TLC) was measured for all pathologically proven HCCs. For each patient, lesion and liver attenuation (HU) were measured by means of a circular region of interest (ROI) placed at an identical position on the images from each imaging phase

(unenhanced, hepatic arterial, hepatic venous and delayed). Liver attenuation was measured as the average value of three different ROIs , the tumor-to-liver contrast (TLC) was calculated during each of the four imaging phases as the difference in attenuation between the lesion and the surrounding liver parenchyma .

These findings were reflected in the TLC results, which showed significantly higher TLC absolute values during the delayed phase (216.1‹10.8 HU) than during the hepatic venous phase (210.5‹10.2 HU) (p,0.001), a finding consistent with greater conspicuity of tumor washout during the delayed phase. Their findings may be partly explained by the analysis of the progression of tumor and liver attenuation over the different imaging phases.

Kamaya et al 2013 state that : A quantitative definition of HCC may minimize inter observer variability and facilitate more accurate diagnosis. They identified 47 liver lesions that were hyperenhancing in the arterial phase from 24 patients who underwent triphasic MDCT . All HCCs were pathologically proven. Regions of interest were obtained of lesions and areas of adjacent liver on arterial, portal venous, and delayed phase images. Enhancement profiles were assessed by three radiologists. There was a statistically significant difference in percentage attenuation ratio (defined as 100 × ratio of attenuation of adjacent liver to that of the HCC lesion) . Their analysis of simple CT attenuation measurements indicates that percentage attenuation ratio offers excellent sensitivity, specificity, PPV, and NPV for HCC detection and very good correlation with radiologists' assessments of washout

On the other hand Haralick et. Al 1973 suggested the use of Gray-tone Spatial-dependence matrices also called Gray-level co-occurrence matrices(GLCM) to extract texture features from an image. Since then, GLCMs became widely used for image texture features extraction in many types of applications .

Mala (2006) demonstrate that The wavelet and the neural network is evaluated in the differential analysis of liver tumors in CT images . The tumors considered in this study are HCC, cholangio carcinoma, Hemangioma and hepatoadenoma. The tumor was automatically extracted from the CT abdominal images and the textural information found was used to train the PNN to classify the tumors. The optimized feature set was selected based on the classification performance of PNN. The performance of the method is assessed for the 105 images. It is found that the LVQ neural network produces an accuracy rate of 83.5%. The PNN network produces an accuracy rate of 90.2%.

Chi et al (2013) aim is to develop an automatic method to facilitate the characterization of focal liver lesions (FLLs) using multiphase computed tomography (CT) . The system was tested on a database of 69 four-phase contrast-enhanced CT scans, consisting of six classes of liver lesions. The texture feature measures the lesion's heterogeneity, including six textural coefficients: Energy, Entropy, Inverse Difference Moment , Inertia, Cluster Shade, and Correlation. The texture coefficients are calculated based on Gray Level Co-occurrence and demonstrate that Multiphase CT images can be used in content-based image retrieval for focal liver lesions (FLL's) categorization and result in good performance in comparison with single-phase CT images . The results were evaluated in terms of the diagnostic accuracy, the receiver operating characteristic (ROC) curve and the mean diagnostic confidence. One radiologist's accuracy improved from 75% to 92%, the area under ROC curves (AUC) from 0.85 to 0.95 (p = 0.081), and the mean diagnostic confidence from 4.6 to 7.3 (p = 0.039). The second radiologist's accuracy did not change, at 75%, with AUC increasing from 0.72 to 0.75 (p = 0.709), and the mean confidence from 4.5 to 4.9 (p = 0.607).

Duda (2006) proposed a new method for characterization of the HCC in multiphase CT images. A database of 495 images (165 images for each acquisition phase) from 22 patients was gathered, Images with the same slice location and corresponding to three typical acquisition moments , ROIs were being recognized: the normal liver and its two main primary malignant lesions: hepatocellular carcinoma and cholangiocarcinoma. were analyzed simultaneously, 4 first order parameters (calculated from the gray level histogram) (*FO*), entropy of image , 8 Run-Length Matrix features (*RLM*), 11 Co-occurrence parameters (*COM*),were obtained from three subsequent acquisition moments (N + A + P) .In this way the texture evolution during the propagation of the contrast product was taken into account. Experiments with various sets of texture parameters and two classification methods showed that the best results were obtained for groups of all texture features . the classification accuracy was greater than 90% for Support Vector Machines and was about 99% for Dipolar Decision Trees) .

Kumar et al 2012 state that : Automatic lesion segmentation, texture feature extraction and classification of malignant and benign tumors from computed tomography (CT) images is proposed ,30 hepatocellular carcinoma and 40 cavernous hemangioma were analyzed, both first order statistic and second order statistic features are extracted from the gray level and contour let detail coefficients. The extracted feature sets are classified by a PNN classifier into benign and malignant with FOS 79% ,GLCM 86% ,CCFOS 93% and CCCM – 94% Results indicate that the contourlet coefficient texture is effective for classifying malignant and benign liver tumors.

A computer-aided diagnostic system has been proposed by Gletsos1 (2001) for the classification of Normal liver, hepatic cysts, Hemangioma, and HCC from abdominal CT , Regions of Interest (ROI's) taken from non-enhanced CT images ,a total of 147 samples, have been used as input to the system. High performance is achieved by the suitability of co-occurrence texture features ,

the application of dimensionality reduction with sequential forward floating selection (SFFS), and the choice of a classifier consisting of three sequentially placed neural networks, have resulted in a total classification performance of 98%, for four classes of hepatic tissue. The application of feature selection with SFFS in the implemented system has resulted not only in high classification performance, but also in reduced complexity and execution times in the order of a few seconds.

Huang 2006 proposed system for diagnoses hepatic tumors using inter pixel textural features within nonenhanced CT. study evaluated 164 liver lesions 80 malignant tumors and 84 hemangiomas). The suspicious tumor region in the digitized CT image was manually selected and extracted as a circular subimage. Proposed preprocessing adjustments for subimages were used to equalize the information needed for a differential diagnosis. The autocovariance texture features of subimage were extracted and a support vector machine classifier identified the tumor as benign or malignant. (The accuracy of the proposed diagnosis system for classifying malignancies is 81.7%, the sensitivity is 75.0%, the specificity is 88.1%, the proposed system is expected to be a helpful tool for classifying benign and malignant tumors in nonenhanced CT images and can provide a second reading to reduce misdiagnosis.

Another study by Smutek (2009) also proposed (CAD) system for focal liver lesions in CT images. The texture analysis methods are used for the classification of hepatocellular cancer and liver cysts in CT contrast enhanced images , The images were taken from 20 adult subjects: 15 subjects with hepatocellular carcinoma and 5 subjects liver cysts. The total number of CT scans processed was 535 images . A total number of 130 spatial and second-order probabilistic texture features were computed from the late post contrast enhancement images. Ensemble of Bayes classifiers was used for the tissue classification. Classification success rate was as high as 100%

The results show the excellent discrimination between hepatocellular carcinoma and liver cysts can be established on the basis as few as one optimal feature among the 130 texture characteristics tested.

Another Computer Aided Diagnosis (CAD) system for the characterization of hepatic tissue from Computed Tomography (CT) images is presented by Mougiakakou1 et al 2003. A total of 147 (ROI.s) were sampled, 76 of which corresponded to healthy controls (C1), 19 to cysts (C2), 28 to hemangioma (C3), and 24 to hepatocellular carcinoma (C4) on abdominal non-enhanced CT images. For each ROI, five distinct sets of texture features are extracted using the following methods: first order statistics, spatial gray level dependence matrix, gray level difference method, Laws. texture energy measures, and fractal dimension measurements. Classification of the ROI is then carried out by a system of five neural networks (NNs), found that : A CAD system based on texture features and a multiple classification scheme for the characterization of four types of hepatic tissue from CT images has achieved a total classification performance of the order of 97%.

Study by Kumar et. al. 2010 proposed a computer-aided diagnostic system for the diagnosis of benign and malignant liver tumors from computed tomography (CT) images using curvelet transform based multi-resolution texture feature extraction and neural network. The input dataset of 70 images are grouped in to two groups of training set and testing set with 35 datasets each. Two kinds of liver diseases were identified including 30 hepatocellular carcinoma and 40 cavernous hemangioma. The experiment results show that The accuracy of classification of tumors using curvelet based texture features extraction is 94.3% while it is only 88.6% using wavelet based. Results obtained were evaluated with the help of radiologists. The system differentiates the tumor with relatively high accuracy and is therefore clinically useful.

A CT liver image diagnostic categorization system was developed by Chen (1998)which consists of a detect-before-extract (DBE) system which finds the liver border without human intervention and a neural network liver classifier for categorization. Classifier uses specially designed feature descriptors to differentiate normal liver, two types of liver tumors, hepatoma and hemangioma. Neural Network is implemented by a modified PNN [MPNN] in combination with feature descriptors which are obtained from Fractal feature information and the gray level co-occurrence matrix. The proposed system was tested with 30 liver cases and revealed to be proficient and very successful. The classification rate obtained is about 83%.

Valavanis et al 2004 Were developed a CAD system aiming to discriminate four hepatic tissue types from non-enhanced CT images. Images taken from both patients and healthy controls were used. A total of 147 free-hand ROIs were sampled and distributed into three disjoint data sets (training, validation, and testing), five sets of features were calculated for each ROI. An ensemble of classifiers has been constructed based on NN leading to a classification performance of 90.63%.

There are only a few studies for multi phasic CT liver segmentation, it has been observed that different algorithms and classification methods have been applied to differentiate liver lesions, Each of them has their own advantages and disadvantages in terms of accuracy, strength or computational cost.

Chapter Three
Materials and Methods

3.1 Material

Helical Multi detector CT scanner Siemens machines (Somatom sensation16 slices 2004); used for collecting data from CT Abdominal images. With .8 second rotation Time , Large SFOV , 120kVp and 320 MA which differ through the phases .

3.2 Design of the study:

This study was an analytical, case control study where the data were collected prospectively and retrospectively.

3.3 Study population

The population of this study was patient with Hepatocellular (HCC) carcinoma underwent abdominal CT Images, (their diagnosis were confirmed by biopsy report) obtained from both gender with their age ranged from 18 years to 92 years old.

Exclusion criteria: The study excluded all pregnant women, patient with Liver Cirrhosis and patient with fatty liver because these conditions alter the sequence of texture analysis consistency.

3.4 Sample size and type:

The data of this study collected from 200 patients confirmed diagnoses with Hepatocellular carcinoma; they were selected randomly from a set of 800 patients present for abdominal CT.

3.5 Place and duration of the study:

This study was carried out in the period from August 2012 to August 2015 in Kingdom of Saudi Arabia- Southern area –Najran City (King Khalid Hospital).

3.6 Methods of data collection

3.6.1 Data collection

Data collected from radiologist reports with Special designed sheet from findings which appear in different CT cuts through the different image phases . The variable data collected from the acquisition of the CT image were: - age, gender, tumor intensity and CT character.

3.6.2 Technique

A database of 600 images (200 images for each acquisition phase) from 200 patients was gathered. The acquisitions were performed with MDCT device and the standardized acquisition protocol was applied: helical scanning, with slice thickness 5 mm for each patient, an appropriate amount of 60% Iodinated Contrast material (about 100 -150 ml), was injected at 4 ml/s rate. The acquisition of the images in the arterial phase started about 20 seconds after contrast injection. Images corresponding to the portal phase were acquired with delay of 50–60 s sequences with single Breath-holds. All images had a size of 512×512 pixels with 8-bit gray levels and were represented in DICOM format.

3.6.3 Methods of analysis:

The CT images were stored in computer disk were viewed by the Radiant, Ant DICOM in computer to selected the axial images that suit the criteria of research population then uploaded into the computer based software Interactive Data Language (IDL) where the DICOM image converted to TIFF format to suit IDL platform . The CT image were read by IDL then the researcher clicks on areas represents the, HCC, liver, kidney and spleen in test group images; in these areas a window of 3×3 pixel were generated and textural feature for the classes center

were generated. These textural features include mean, variance, Skewness, Kurtosis, energy, and entropy. These features were assigned as classification centre used by the Euclidian distances to classify the whole image. The algorithm scans the whole image using a window; 3×3 pixels and computes the above mentioned textural features and then computes the distance (the Euclidean distance) between the calculated features during the scanning and the class's centers and assigns the window to the class with the lowest distance. Then the window interlaced one pixel and the same processes started over again till the entire image were classified and classification maps were generated. After all images were classified the data concerning the normal tissues (liver, kidney and spleen) and tumor (HCC) entered into SPSS with its classes to generate a classification score using stepwise linear discriminate analysis; to select the most discriminate features that can be used in the classification of abdominal tissues in CT images. Where scatter plot using discriminate function were generated as well as classification accuracy and linear discriminate function equations to classify the abdominal tissues into the previous classes without segmentation process for unseen images in routine work. The delineation of HCC done by furthers processing of the classification using region label function to segment the HCC tumor from the other classes and convert the segmented HCC from classification map with pseudo-color to binary image to extract (segment) the HCC tumor from the whole original image. Then by applying Sobel function the outline of the binary image was generated and the spatial location of the pixels was used to delineate the HCC on the original image using read line. Similar method was obtained for the same set using grey scale as input instead of the texture, where the grey level were extracted from all phases (plain, arterial and venous). This method was done first to explore the potential of linear attenuation potential before devoting the whole process to the first order textural features.

3.7- Ethical issue:

Ethical approval was carefully considered at the time of the study; Permission was taken from the head of the radiology and imaging department of King Khalid hospital to perform the study. All patients were informed to obtain their consent before the exam and their information's will be used in this study.

Chapter Four

Result

The study include 200 patient who were diagnosed with Hepatocelluler carcinoma, in multi-phasic CT scanner. The main objective of this study was to characterize the HCC using texture analysis and grey level intensity so far for the classification and delineation of the HCC and liver in CT images. The result of this study represented in figures and tables.

Table (4-1) and Figure (4-1) Shows the gender distribution among hepatocellular carcinoma patient's , reflect that the higher percentage of the disease associated with male , 147 of 200 HCC patients (73.5%) , while the affected female were 53 0f the 200 sample (26%) . Table (4-2) and Figure (4-2) Shows the age distribution of the patient Ranged from 18 to 92 year , Minimum age range was 10-20 , and Maximum age range was 91-100 . Table (4-3) Figures (3,4,5) Shows the differences in the mean intensity values of the five selected abdominal classes on Tri-phasic CT for plain, arterial and venous phase The mean intensity values for the HCC during the precontrast , HAP and PVP were, 116.8 , 135.5 and 118 respectively .The highest intensity value were measured during the HAP , While that the mean intensity for the liver parenchyma during the precontrast , HAP and PVP were 138.9 , 145.6 and 174.9 respectively , The highest intensity value were measured during the PVP **.** While Figure (4-6) lines graph demonstrate the parallel of the mean intensity of the selected classes on plain, arterial and venous phase as group . The Figure (4-7) A ,B and C illustrate the sequences of HCC delineations then the extraction followed by classification of the liver respectively using Euclidian distance .

Figure 4-8 error bar plot for the entropy in unenhanced phase , Figure 4-9 error bar plot for the entropy in arterial and Figure 4-10 error bar plot for the entropy in the venous phase , textural features that selected by the linear stepwise discriminate function as a discriminate feature where it discriminate clearly between the HCC, liver , kidney and spleen.

Figure 4-11 Scatter plot generated using discriminate analysis function for four classes represents: HCC, Liver, Kidney and Spleen

Table 4- 4 Classification score matrix generated by linear discriminate analysis for the scatter plot shown in Figure 4-8 with classification accuracy of 89.1% . The Figure (4-12, 13) A ,B and C illustrate the sequences of HCC delineations then the extraction followed by classification of the liver using Euclidian distance and linear discriminate analysis respectively .

Table (4.1) Shows Gender distribution of the HCC patient

Gender	Frequency	Percent
M	147	73.5%
FE	53	26.5%
Total	200	100%

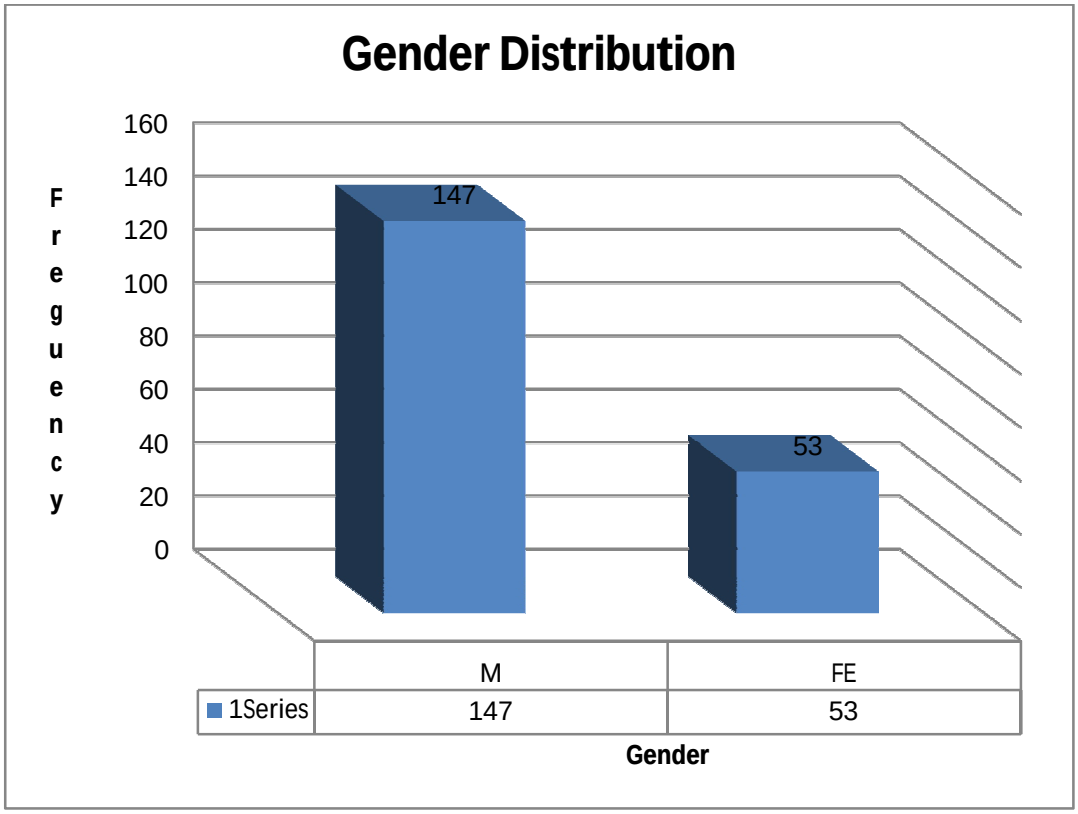

Figure (4.1) Show Gender distribution of the HCC patient

Table (4.2) Shows ages distribution of HCC patient (year)

Age	Frequency	Percentage
10 -20	1	.5%
21 - 30	4	2%
31 - 40	8	4%
41 - 50	23	11.5%
51 - 60	48	24%
61 - 70	69	34.5%
71 - 80	39	19.5%
81 - 90	6	3%
91 - 100	2	1%
Total	200	100%

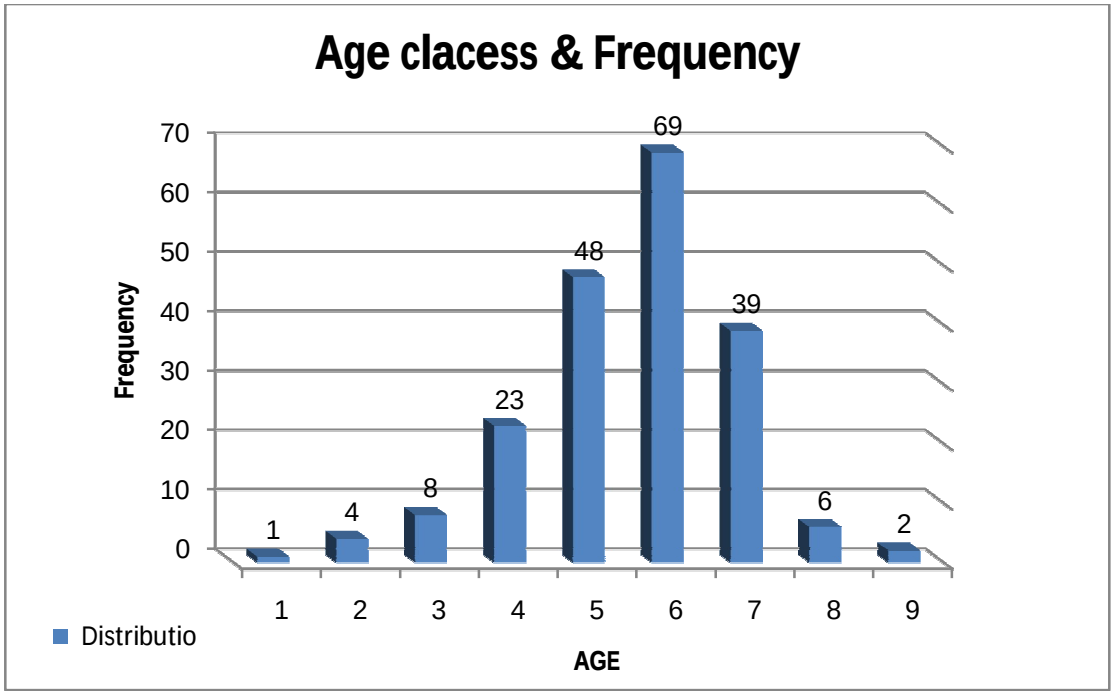

Figure (4.2) Shows age distribution of HCC patient (year)

Table (4-3) Show the mean intensity of the selected abdominal classes on CT for plain, arterial and venous phase

Organ	Plain	arterial	venous
Stomach	121.1875	172.68	218.51
Spleen	133.3990	175.30	188.91
Kidney	123.1515	207.78	225.69
Liver	138.9495	154.64	174.96
HCC	116.8434	135.46	118.40

Table 4- 4 Classification score matrix generated using Euclidian distance analysis with classification accuracy of 70.3%

	Predicted Group Membership				
Original	**HCC**	**Kidney**	**Liver**	**Spleen**	**Total**
HCC	**41.1**	**27.0**	**14.9**	**17.o**	**100.0%**
Kidney	**12.8**	**82.2**	**0.0**	**0.0**	**100.0** %
Liver	**10**	**0.0**	**87.7**	**2.4**	**100.0** %
Spleen	**7**	**12**	**4.3**	**76.7**	**100.0** %

classification accuracy 70.3

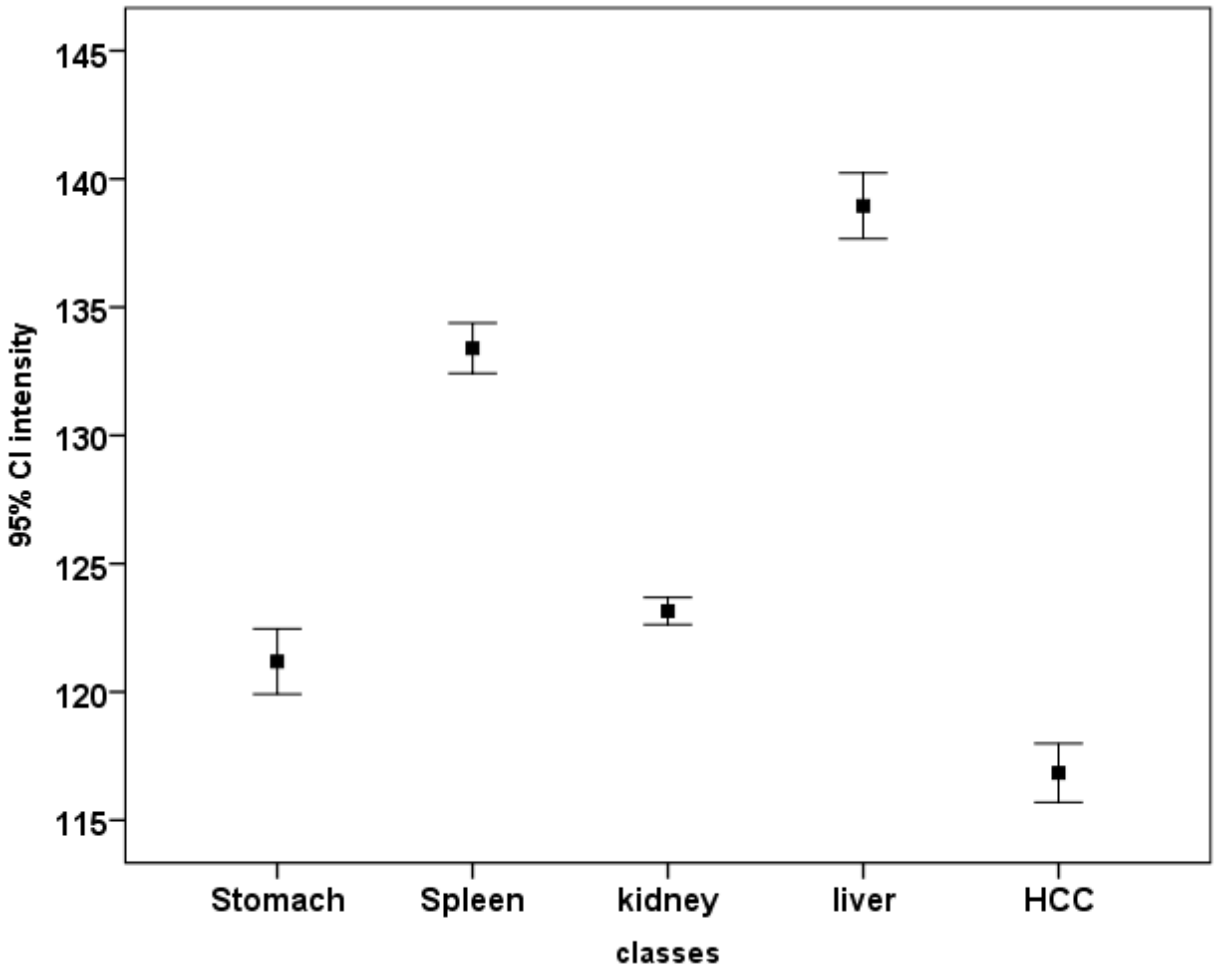

Figure (4-3) Error bar plot of the mean intensity of the selected classes on plain CT

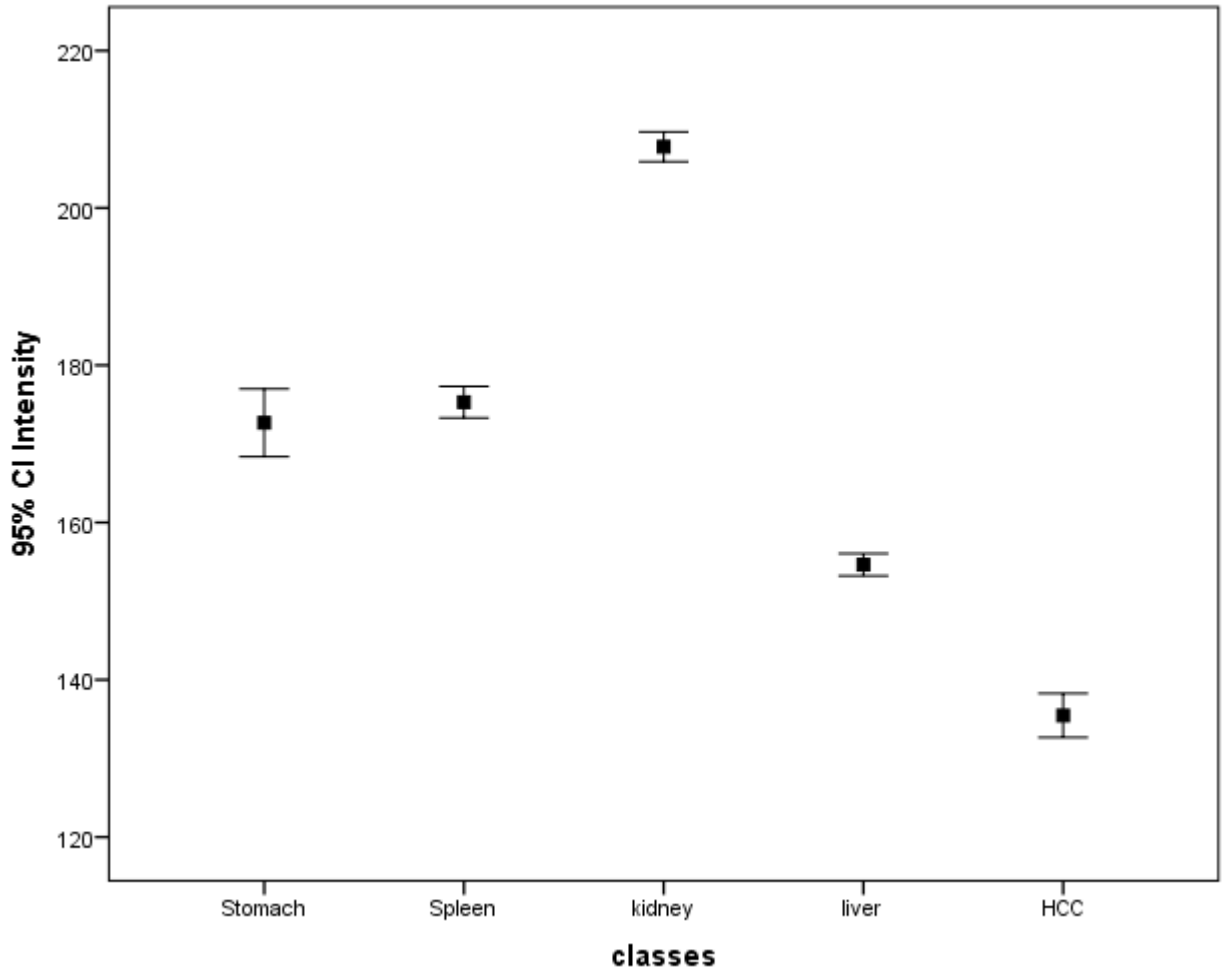

Figure (4-4) Error bar plot of the mean intensity of the selected classes on CT arterial phase

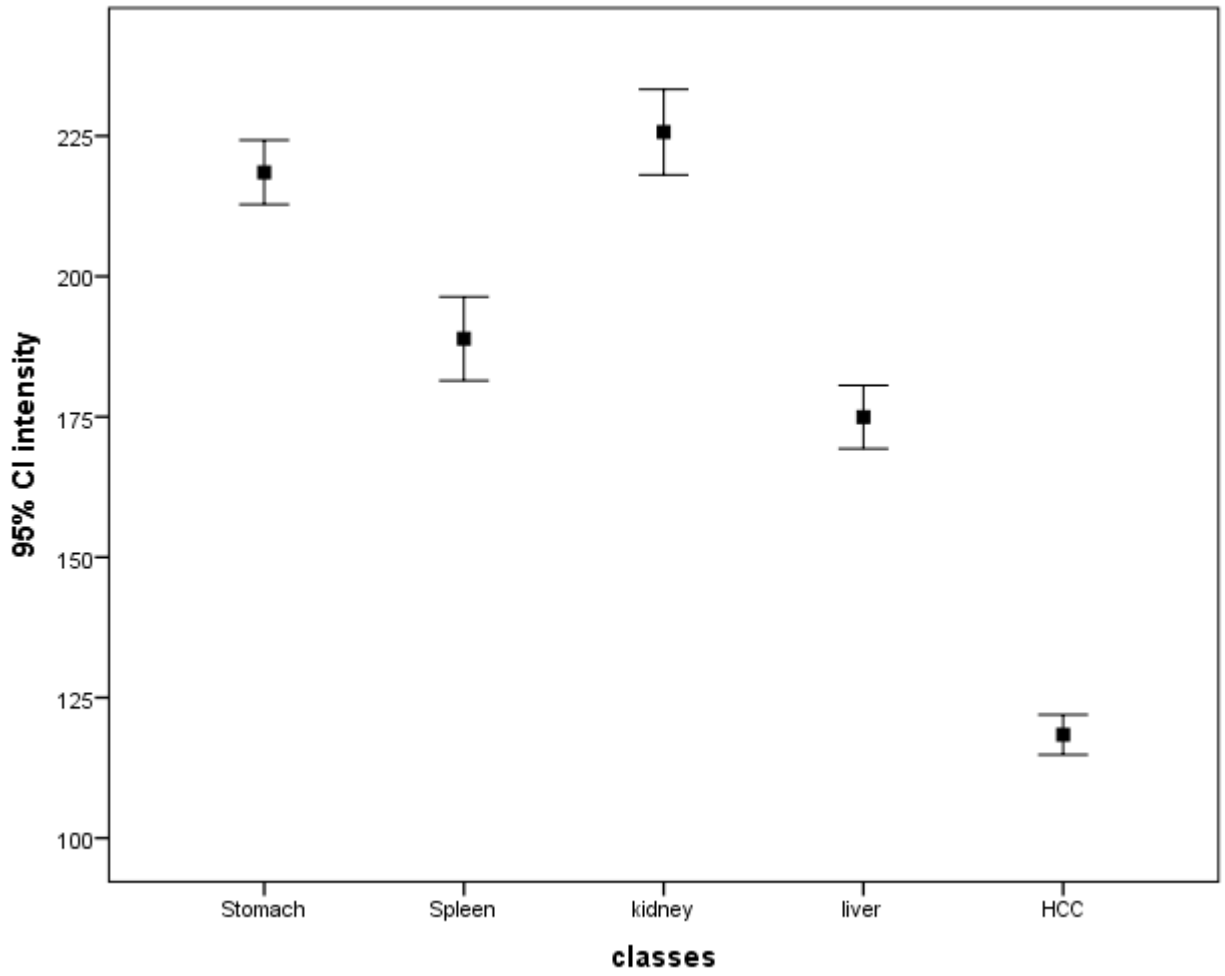

Figure (4-5) Error bar plot of the mean intensity of the selected classes on CT venous phase

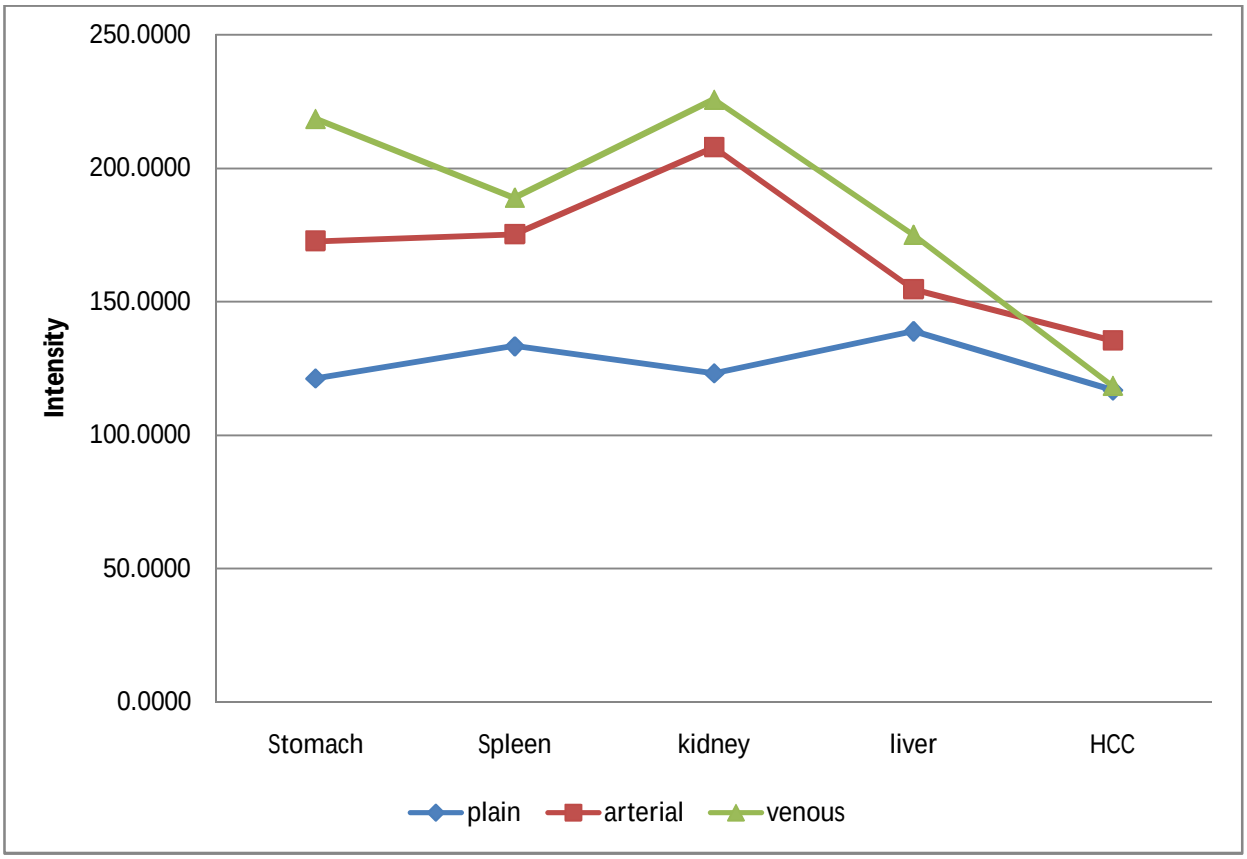

Figure (4-6) lines graph of the mean intensity of the selected classes on CT for plain, arterial and venous phase

(A)

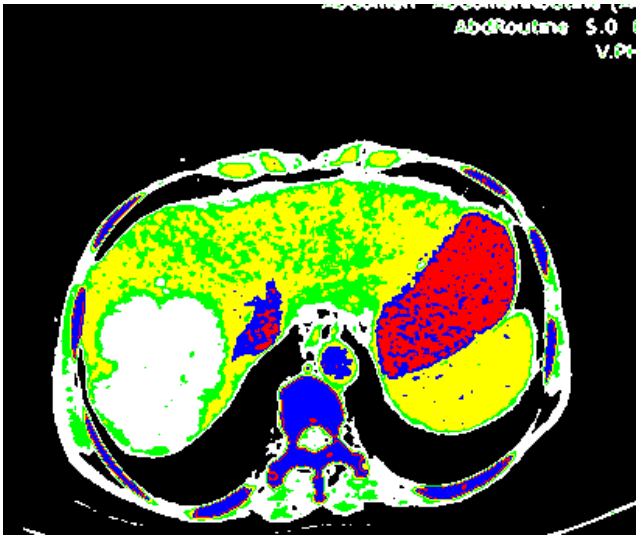

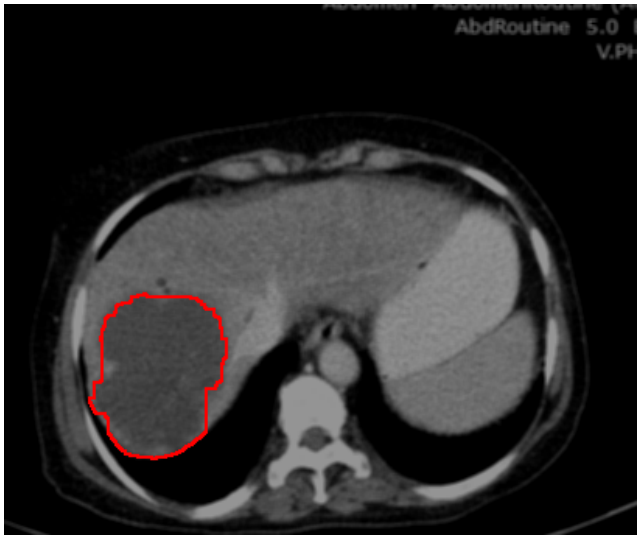

(B)

(C)

Figure 4-7(A)an original axial CT image (B) classification map of the original image using Euclidian distance, (C) an original image with tumor region delineated

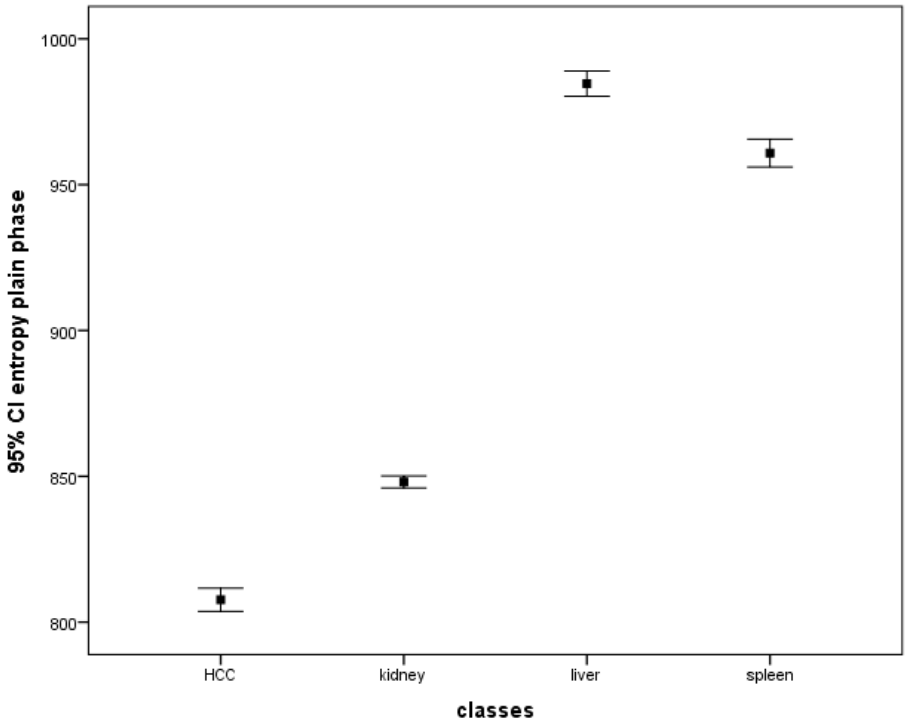

Figure 4-8 error bar plot for the entropy in unenhanced CT phase

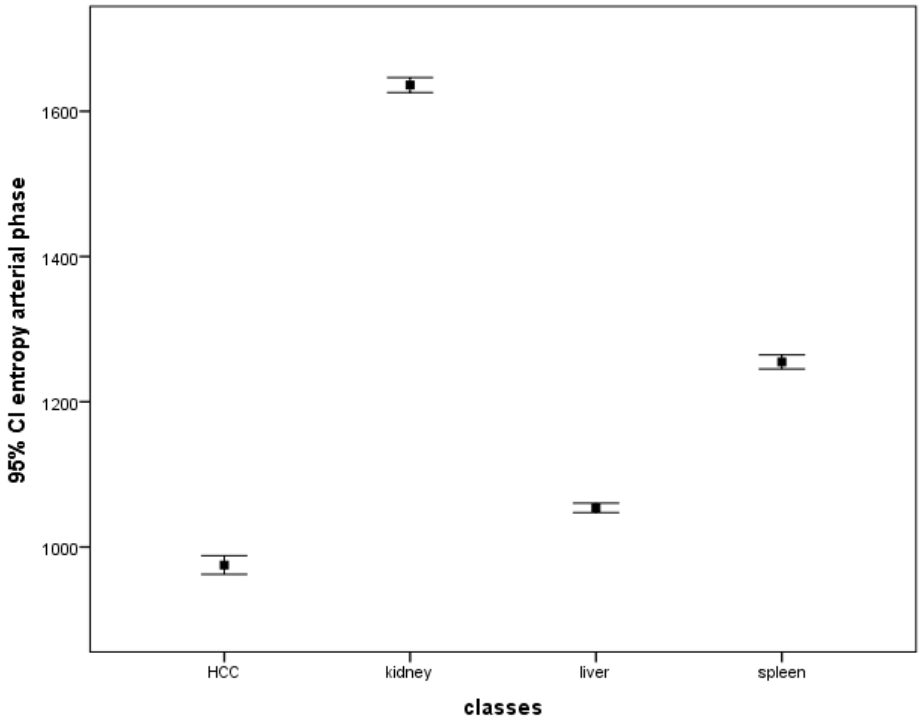

Figure 4-9 error bar plot for the entropy in arterial CT phase that selected by the linear stepwise discriminate function as a discriminate feature .

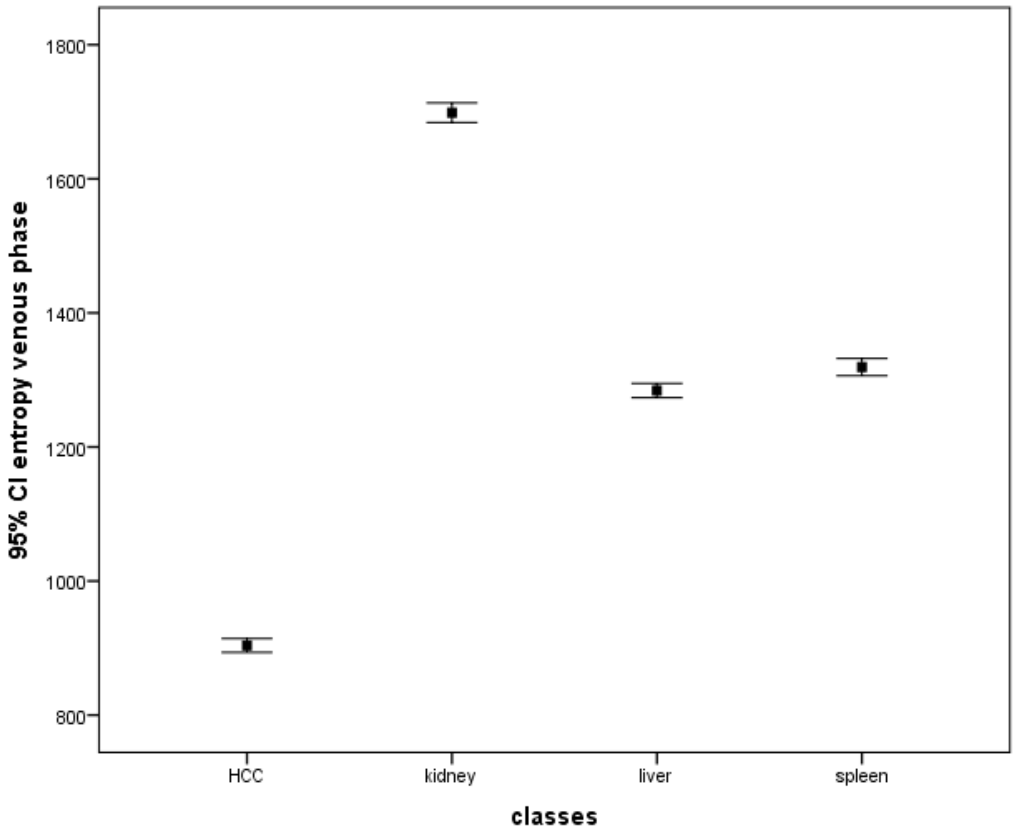

Figure 4-10 error bar plot for the entropy in the venous phase ,that selected by the linear stepwise discriminate function as a discriminate feature where it discriminate between all features between HCC, liver , kidney and spleen

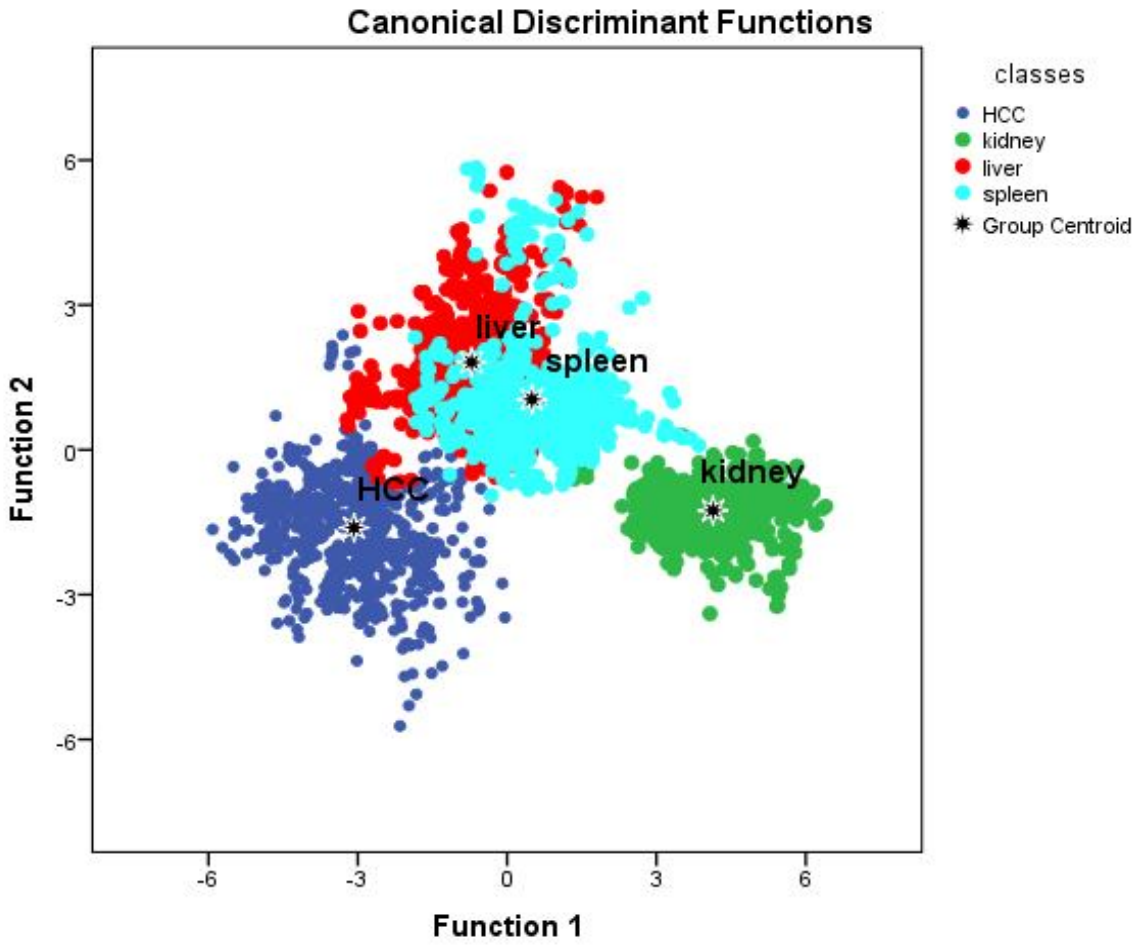

Figure 4-11 Scatter plot generated using discriminate analysis function for four classes represents: HCC, Liver, Kidney and Spleen

Table 4- 5 Classification score matrix generated by linear discriminate analysis for the scatter plot shown in Figure 2 with classification accuracy of 89.1%

classless		Predicted Group Membership				
		HCC	kidney	liver	spleen	Total
Original	HCC	**96.5**	0.0	1.4	2.1	100.0%
	kidney	0.0	**97.9**	0.6	1.4	100.0%
	liver	2.2	0.0	**83.9**	13.9	100.0%
	spleen	0.0	1.5	20.5	**78.0**	100.0%

89.1% of original grouped cases correctly classified (accuracy).

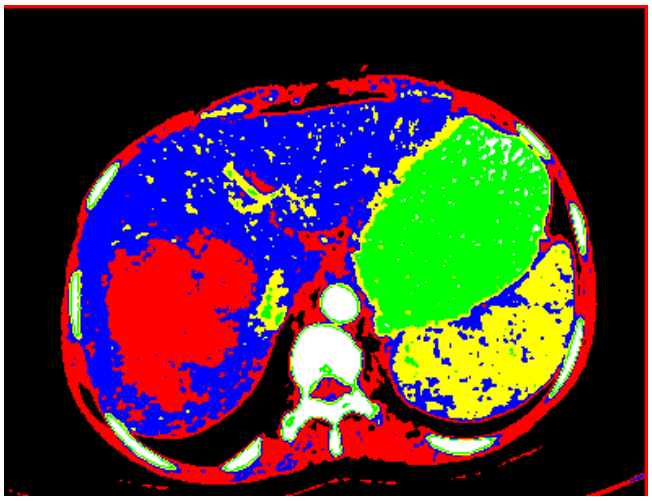

(A)

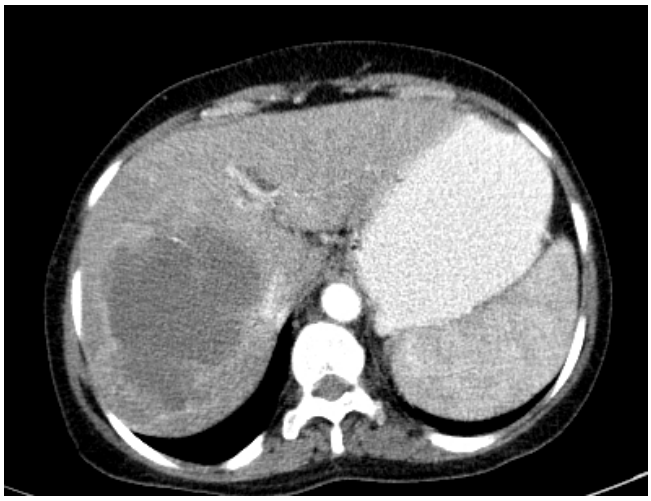

(B)

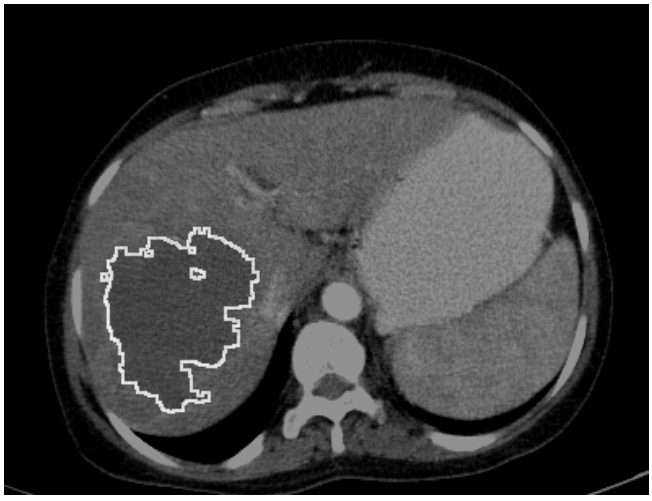

©

The Figure (4-12) A ,B and C illustrate the sequences of HCC delineations then the extraction followed by classification of the liver using Euclidian distance and linear discriminate analysis respectively .

(A)

(B)

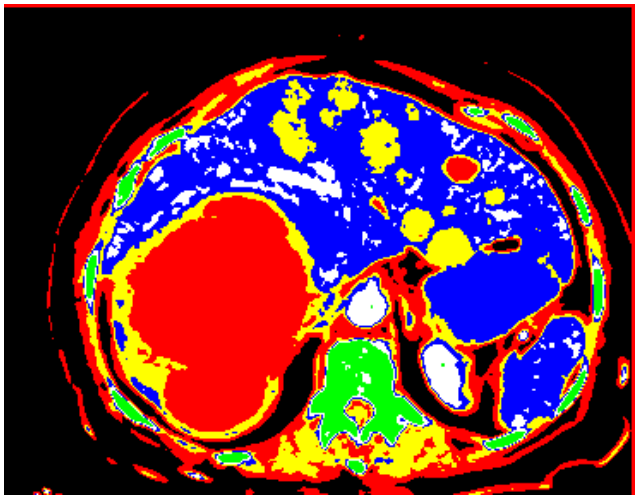

(C)

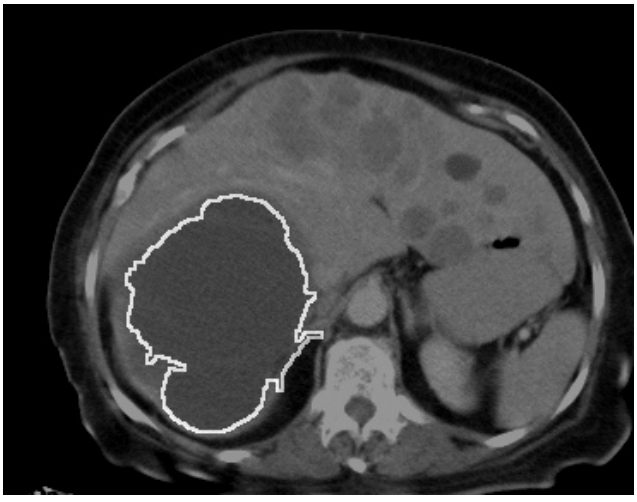

Figure 4-13(A)an original axial CT image (B) classification map of the original image using Euclidian distance, (C) an original image with tumor region delineated

Chapter Five

Discussion, conclusions and recommendations

5.1 Discussion:

The use of medical imaging and tissue characterization techniques is becoming increasingly popular in diagnosis, treatment and research. However, in the case of liver disease, characterization of hepatic lesions from Computed Tomography (CT) is troublesome, even for experienced radiologists, and often requires confirmation by biopsies, or other invasive techniques . To overcome this, a variety of computer-aided diagnostic systems have been proposed. The system involves use of different measures, such as texture features, grey scale, fractal dimension estimators or shape descriptors, combined with a classifier . This is analytical study, performed for 200 patient , male and female who are presented for abdomen - CT for liver abdominal using multidetector helical CT Scan (MDCT) . In this study there were 18 features extracted from Triphasic CT images using 3×3 window. Three of them showed well classification with the predefined classes (HCC, normal Liver , kidney and spleen) .These textural features include mean, variance, Skewness, Kurtosis, energy, and entropy.

Table (4-1) and Figure (4-1) shows Gender distribution among hepatocellular carcinoma patient's , reflect that the higher percentage of the disease associated with male , 147 of 200 HCC patients (73.5%) , while the affected female were 53 of the 200 sample (26%) . And Table (4-2) and Figure (4-2) shows the age distribution of the patient Ranged from 18 to 92 year , demonstrate that the incidence of the HCC increased with ageing , and the higher affected age between 61 to 70 year , this present agrees with the study by (Bosch 1997) who state that The

incidence of hepatocellular carcinoma increases progressively with advancing age in all populations, although it tends to level off in the oldest age groups and is rare in children . Figure (4-3) shows Our analysis of simple measurements of intensity explained by the analysis of the progression of HCC , liver and other abdominal classes over the different imaging phases which demonstrate that , on the pre-contrast scan all HCC lesions were either isodense or hypodense relative to surrounding liver parenchyma., while Figure (4-4) shows the arterial phase, HCC intensity values were reach their maximum enhancement with mean intensity of (135) , but it is still lower than the surrounding liver parenchyma ,therefore the tumor appear as hypoattenuating, while during the PVP the intensity of the tumor were decreased and clear washout during the venous phase is detected with mean intensity of (119) , Figure (4-5) . In contrast the intensity of surrounding liver were increased during the HAP , but they were reach their maximum enhancement during the PVP with mean intensity of (174.9) Previous authors have suggested that this finding is a consequence of the intralesional enhancement of the contrast medium during the arterial phase .

The enhancement difference is thought to be related to the differences in blood supply. HCCs receive blood primarily from the hepatic arteries and therefore tend to enhance more avidly than background liver during late arterial phase imaging, whereas the normal liver receives approximately 25% of its blood supply from the hepatic artery and 75% from the portal vein during the portal venous phase of contrast enhancement, the liver continues to enhance, and the lack of portal venous blood supply to HCCs results in the characteristic washout in the portal venous phase and especially in the delayed phase. In addition, the liver parenchyma is often fibrotic in patients with HCC. Because fibrotic tissues are known to wash in and wash out

slowly, this may also contribute to the hypodense appearance of HCCs in the portal venous and delayed phases .

In our study most of the HCC tumors were large in size , (mean size 6cm) and these most likely associated with necrotic tissues, therefore, blood supply will be poor during the arterial phase this contribute to the hypodense appearance of HCCs in the arterial phase Figure (4-6).

Same result achieved by Monzawa et al 2007 , who state that Some HCCs, especially small or well-differentiated lesions, may not be hyperenhancing on arterial phase images, only 58% of HCCs < 2 cm were hypervascular on the arterial phase Conversely, a minority of hypervascular HCCs may not exhibit washout on portal venous or delayed phase image . The Figure (4-7 A ,B and C) illustrate the sequences of HCC delineations A)an original axial CT image (B) classification map of the original image using Euclidian distance, (C) an original image with tumor region delineated .

Figures 4-8 ,9,and 10 error bar plot for the entropy in the plain , arterial and venous phase ,that selected by the linear stepwise discriminate function as a discriminate feature where it discriminate between all features between HCC, liver , kidney and spleen . Of the 18 extract features three FOS features,(entropy in unenhanced plain phase , entropy in the arterial phase and entropy in the venous phase) were computed from gray level histogram and the results are represented that there is a well concentration of features around the class centers which give a remarkable difference among the four classes especially between the HCC and normal liver tissues in the entropy in plain, arterial and venous phases . However , No clear difference in the entropy was seen between the HCC and liver in the arterial phase (Fig 4-9).

Among all image phases, HCC reveal different value which, was low and relatively static (low entropy variation).

Figure (4-11) shows that linear discriminate analysis were used to classify the HCC , and normal abdominal tissues, so the features of the classified regions of the whole images (as raw data) were classified furthers. The result of the classification showed that the HCC were classified well from the normal liver tissues even though it has characteristics similar to surrounding tissue , and the texture reveal a different underlying pattern compared to the liver and other abdominal tissues with classification sensitivity 96.5% , and the combination of the texture features throughout the different triphasic image phases provides the highest predictive overall accuracy of 89.1 % using stepwise linear discriminant analysis Table (4-5) .Same method achieved by Duda 2006 which Characterize the HCC texture from multiphase CT images from a database of 495 images from 22 patients. Images with the same slice location and corresponding to three typical acquisition moments were analyzed simultaneously. In this way the texture evolution during the propagation of the contrast product was taken into account. The method was applied to recognizing normal liver and its two main primary tumors. classification methods showed that the best results were obtained for groups of all texture features . the classification accuracy was greater than 90% for Support Vector Machines and was about 99% for Dipolar Decision Trees) .

The Figure (4-12,13 A ,B and C) illustrate the sequences of HCC delineations then the extraction followed by classification of the liver using Euclidian distance and stepwise linear discriminate analysis respectively

Finally HCC and other abdominal organ in CT images for simplicity can be diagnosed and classify by using the following simple equation after extracting the associated features using a window of 3×3 pixel from the region of interest; the biggest classification score assume the tissue type :

$$HCC = (entropy\_P\,l \times 0.28) + (entropy\_Ar \times 0.05) + (entropy\_Vn \times 0.04 - 158.92$$

$$Kidney = (entropy\_P\,l \times 0.30) + (entropy\_Ar \times 0.10) + (entropy\_Vn \times 0.08) - 264.11$$

$$Liver = (entropy\_P\,l \times 0.34) + (entropy\_Ar \times 0.06) + (entropy\_Vn \times 0.06) - 237.11$$

$$Spleen = (entropy\_P\,l \times 0.33) + (entropy\_Ar \times 0.07) + (entropy\_Vn \times 0.05) - 243.78$$

Excellent discrimination between hepatocellular carcinoma and other abdominal organ can be established based on the texture characteristics and this serves as a second method to perform more characterization of the tumor.

5-2 Conclusions :

- The texture reveal a different underlying pattern of the HCC compared to the liver and other abdominal tissues with classification sensitivity 96.5% , and the combination of the texture features throughout the different triphasic image phases provides the highest predictive overall accuracy of 89.1 % using stepwise linear discriminant analysis .
- This study dictate that texture analysis is superior to visual perception system where texture reveals the change and the difference of the image pattern objectively in respect to the ground truth.
- Gray level intensity values can be used as a valuable quantitative tool that would be helpful in improving the confidence in HCC diagnosis as well as facilitating more accurate diagnosis.
- In this study the incidence of Hepatocelluler carcinoma is more common in male than female (73.5 %: 26.5%) & increases progressively with ageing in all populations .

5-3 Recommendations

- Existing techniques can be applied to classify and differentiate other types of liver lesions
- More texture features and techniques can be used to improve the performance.
- Texture analysis can be carried out in all image slices where the tumor were visible therefore to get volume of the tumor and this can be used for planning process of radiotherapy treatment.
- . Study can also be done in depth for other types of medical images like MRI .
- Initiation of image processing unit in the radiology department can help a lot in activation of image processing projects.

REFERENCES :

- Arguedas MR, Chen VK, Eloubeidi MA, et al. Screening for hepatocellular carcinoma in patients with hepatitis C cirrhosis: a cost-utility analysis. Am J Gastroenterol 2003;98:679–690.

- Ahmet Gurakar, James P. Hamilton, et al Hepatocellular Carcinoma (Liver Cancer) Copyright 2001-2013 | All Rights Reserved., Baltimore, Maryland 21287

- Bonilha L, Kobayashi E, Castellano G, et al. Texture analysis of hippocampal sclerosis.Epilepsia 2003;44:1546–50.9.

- Bruno A., Collorec R., Bezy-Wendling J., Reuze P., Rolland Y.: Texture analysis in medical imaging, In: Roux C., Coatrieux J. L. (Eds.): Contemporary Perspectives in Three-dimensional Biomedical Imaging, IOS Press 1997, 133–164

- Bosch FX, Ribes J, Borras J. Epidemiology of primary liver cancer. Semin Liver Dis 1999; 19:271-85.

- Byung Ihn Choi • Jeong Min Lee . Imaging diagnosis and staging of hepatocellular carcinoma, J Hepatobiliary Pancreat Sci (2010) 17:369–373 .

- Chii-Jen Chen and You-Wei Wang, "A Preoperative 3D Computer-Aided Segmentation and Reconstruction System for Lung Tumor ", Journal of Communication and Computer, Volume 9, April 2012, pp. 422-425.

- Chikui, T., K. Tokumori, K. Yoshiura, K. Oobu, S.Nakamura, K. Nakamura (2005), *Sonographic characterization of salivary gland tumors by fractal analysis* , Ultrasound in Medicine and Biology, Vol. 31, No. 10, pp. 1297–1304

- Chiaramonte M, Stroffolini T, Vian A, et al. Rate of incidence of hepatocellular carcinoma in patients with compensated viral cir-rhosis. Cancer 1999; 85:2132-7.

- Chen E. L., Chung P. C., Chen C. L., Tsai H. M., Chang C. I.: An automatic diagnostic system for CT liver image classification. IEEE Transactions on Biomedical Engineering 1998, 45(6), 783–794.

- Chen EL, Chung PC, Chen CL, Tsai HM, Chang CI (1998) An Automatic Diagnostic System for CT Liver Image Classification. IEEE Transactions on Biomedical Engineering 45:6:783-794

- Colli A, Fraquelli M, Casazza G, et al. Accuracy of ultrasonography,spiral CT magnetic resonance, and alpha-fetoprotein in diagnosing hepatocellular carcinoma: A systematic review. Am J Gastroenterol 2006; 101:513-23.

- Cher Heng Tan et al , Wash-out of Hepatocellular Carcinoma: Quantitative Region of Interest Analysis on CT , , Ann Acad Med Singapore 2011;40:269-75.

- Chen, C. J., Chen, D. S., *Hepatology* , 2002, *36*, 1046–1049.

- Choi D, Kim SH, Lim JH, et al. Detection of hepatocellular carcinoma: combined T2-weighted and dynamic gadolinium-enhanced MRI versus combined CT during arterial portography and CT hepatic arteriography. J Comput Assist Tomogr 2001;25: 777–785.

- D. Duda, M. Krętowski, J. Bezy-Wendling , Texture Characterization for Hepatic Tumor Recognition in Multiphase CT , Biocybernetics and Biomedical Engineering, Volume 26, Number 4,2006, pp. 15–24

- Dekker A, Ten Kate FJ, Terpstra OT, et al. Cholangiocarcinoma associated with multiple bile duct hamartomas of the liver. Dig Dis Sci 1989; 34:952-8.

- Dushyant V. Sahani, Sanjeeva P. Kalva, “Imaging the Liver” The Oncologist, 2004, 9: 385-397.

- Eldad S. Bialecki & Adrian M. Di Bisceglie, Diagnosis of Hepatocellular Carcinoma. 2005 Taylor & Francis group LTd, pp 27-36

- E. Edward bittar, The liver in biology and disease, Elsevier ltd, The Netherlands, 2004,120.

- Faller, The Human Body © 2004 Thieme All rights reserved. Usage subject to terms and conditions of license.

- Furlan et at , Hepatocellular carcinoma in cirrhotic patients at multidetector CT: hepatic venous phase versus delayed phase for the detection of tumor washout , The British Journal of Radiology, 84 (2011), 403–412

- Glestos M, Mougiakakou SG, Matsopoulos GK., Nikita KS, Nikita, AS, Kelekis D (2001) Classification of hepatic lesions from CT images using texture features and neural networks. In: Proc. Of 23rd Annual EMBS International Conference of IEEE on Engineering in Medicine and Biology Society 3: 2748–2752 .

- Gunasundari S , Janakiraman A Study of Textural Analysis Methods for the Diagnosis of Liver Diseases from Abdominal Computed Tomography ,*International Journal of Computer Applications (0975 – 8887) Volume 74– No.11, pp 7-13 July 2013* .

- G. Lowitz, "Can a Local Histogram Really Map Texture Information?", *Pattern Recognition*, 16, 2, 1983, 141-147.

- Gunasundari S &Janakiraman S , A Study of Textural Analysis Methods for the Diagnosis of Liver Diseases from Abdominal Computed Tomography *International Journal of Computer Applications (0975 – 8887) Volume 74– No.11, July 2013.*

- Galloway M. M.: Texture analysis using gray level run lengths. Computer Graphics and Image Processing 1975, 4, 172–179.

- H.M. Taylor, P.R. Ros, .Hepatic Imaging: An Overview,. *Radiologic Clinics of North America*, vol.36, no. 2, March 1998.

- Haralick RM, Shanmugam K, Dinstein I. Textural features for image classification IEEE Transactions on Systems, man and cybernetics 1973; 3(6): 610–621.

- Huang GT, Sheu JC, Yang PM, Lee HS, Wang TH, Chen DS. Ultrasound-guided cutting biopsy for the diagnosis of hepatocellular carcinoma –. J Hepatol 1996;25:334–8.

- http://www.intechopen.com/books/biomedical-imaging/texture-analysis-methods-for-medical-image characterisation.

- Harold ellis , Clinical Anatomy ,Arevision and applied anatomy for clinical students, eleventh edition , © 2006 Harold Ellis Published by Blackwell Publishing Ltd, 93-94

- Ioannou G, Splan M, Weiss N, et al. Incidence and predictors of hepatocellular carcinoma in patients with cirrhosis. Clin Gastro-enterol Hepatol 2007; 5:938-45.

- Isaacs H Jr. Fetal and neonatal hepatic tumors. J Pediatr Surg 2007; 42:1797-803.

- Josep M. Llovet (EASL); Michel Ducreux (EORTC). EASL–EORTC Clinical Practice Guidelines: Management of hepatocellular carcinoma, Journal of Hepatology 2012 vol. 56 j 908–943.

- Julesz, B. (1975). Experiments in the visual perception of texture. *Scientific American*, Vol

- Kudo M. Imaging diagnosis of hepatocellular carcinoma and premalignant/borderline lesions. Semin Liver Dis 1999; 19:297- 309.

- Kulkarni PB, Beatty E Jr. Cholangiocarcinoma associated with biliary cirrhosis due to congenital biliary atresia. Am J Dis Child 1977; 131:442-4.

- Kew MC. Tumour markers of hepatocellular carcinoma. J Gastroenterol Hepatol 1989; 4:373-84.

- Kumar SS, Moni RS, Rajeesh J (2012) Liver tumor diagnosis by gray level and contourlet coefficients texture analysis. International Conference on Computing, Electronics and Electrical Technologies 557 – 562 .

- Kamaya1 Liu YI Yueyi I. Liu1 Lewis K. Shin1,2 R. Brooke Jeffrey1 Aya, Shin LK, Jeffrey RB, Quantitatively Defining Washout in Hepatocellular Carcinoma AJR:200, January 2013.

- Luca A, Milazzo M, Caruso S, et al. Hepatic nodules detected in cirrhotic patients using high-performance multidetector computed tomography (MDCT) and magnetic resonance imaging (MRI): A radiological-pathological correlation on explanted livers. J Hepatol 2007; 46(Suppl 1):S37.

- M. Levine, *Vision in Man and Machine*, McGraw-Hill, 1985.

- Mazzanti R, Gramantieri L, Bolondi L. Hepatocellular carcinoma: Epidemiology and clinical aspects. Mol Aspects Med 2008; 29: 130-43.

- M. Gletsos1, S. G. Mougiakakou1*, G. K. Matsopoulos1, K. S. Nikita1, A. S. Nikita2, D. Kelekis2, classification of hepatic lesions from ct images using texture features and neural networks, international conference of the IEEE Engineering in Medicine and Biology Society, held in Istanbul, Turkey October 25-28, 2001,

- Mala K, Sadasivam V, S.Alagappan (2006 b) Neural Network based Texture Analysis of Liver Tumor from Computed Tomography Images. International Journal of Biological and Life Sciences 2:1:33-40 .

- Marrero JA, Hussain HK, Nghiem HV, et al. Improving the prediction of hepatocellular carcinoma in cirrhotic patients with an arterially enhancing liver mass. Liver Transpl 2005;11:281–289.

- Madabhushi, A., M.D. Felman, D.N. Metaxas, J. Tomaszeweski, D. Chte (2005), *Automated Detection of Prostatic Adenocarcinoma From High-Resolution Ex Vivo MRI*, IEEE .Transactions on Medical Imaging, December 2005, pp. 1611-1626 .

- Monzawa S, Ichikawa T, Nakajima H, Kitanaka Y, Omata K, Araki T. Dynamic CT for detecting small hepatocellular carcinoma: usefulness of delayed phase imaging. *AJR* 2007; 188:147–153.

- *Omar Faiz ,David Moffat* Anatomy at a Glance 2002 by Blackwell Science Ltd, *pp 31-45*

- Phillip E. Pack, , and Steven Bassett , Cliff sNotes® Anatomy & Physiology Quick Review, 2nd Edition 2011, Published by: Wiley Publishing, PP 275-276.

- Olfa Ben Sassi1 et al , improved spatial gray level dependence matrices for texture analysis , International Journal of Computer Science & Information Technology (IJCSIT) Vol 4, No 6, December 2012, pp 209- 219

-. Parkin D, Muir C, Whelan S. Cancer incidence in five continents. IARC publication no. 120. Lyon, France: IARC; 1997.

- Parkin DM, Bray F, Ferlay J, Pisani P. Global cancer statistics, 2002. *CA Cancer J Clin* 2005; 55:74–108

- Parkin, D. M., *Lancet Oncol.* 2001, *2*, 533–543.

- Valerie C. Scanlon , Essentials of anatomy and physiology/ 5th ed..chapter 13 pp 301 Copyright © 2007 by F. A. Davis Company

- Sleisenger and Fordtran's Gastrointestinal and Liver Disease , Ninth Edition Chapter 94, 1569-1592.e6 , Copyright © 2010, by Saunders, an imprint of Elsevier Inc.

- Yalcin S. Diagnosis and management of cholangiocarcinomas: A comprehensive review. Hepatogastroenterology 2004; 51:43-50.

- Raza SA, Clifford GM, Franceschi S. Worldwide variation in the relative importance of hepatitis B and hepatitis C viruses in hepa-tocellular carcinoma: A systematic review. Br J Cancer 2007; 96: 1127-34.

- Willatt JM, Hussain HK, Adusumilli S, Marrero JA. MR Imaging of hepatocellular carcinoma in the cirrhotic liver: Challenges and controversies. Radiology 2008; 247:311-30.

- Yu SC, Yeung DT, So NM. Imaging features of hepatocellular car-cinoma. Clin Radiol 2004; 59:145-56.

- Takayasu K. Hepatic angiography. In: Okuda K, Tabor E, editors. Liver Cancer. New York: Churchill Livingstone; 1997. pp 347-59.

- William Henry Nailon (2010). Texture Analysis Methods for Medical Image Characterisation, Biomedical Imaging, Youxin Mao (Ed.), ISBN: 978-953-307-071-1, InTech, Available from:

- Tuceryan, M. & Jain, A.K. (1998). Texture analysis. In: Chen, C.H; Pau, L.F. & Wang, P.S.P., (eds). *The handbook of pattern recognition and computer vision*. 2nd ed. World Scientific Publishing Co., ISBN 9-810-23071-0, Singapore .

- Yanling Chi et al , Content-based image retrieval of multiphase CT images for focal liver lesion characterization , Medical Physics, Vol. 40, No. 10, October 2013- 103502/13

- Yu-Len Huang, PhD, Jeon-Hor Chen, MD, and Wu-Chung Shen, MD,Diagnosis of Hepatic Tumors With Texture Analysis in Nonenhanced Computed Tomography Images1, Acad Radiol 2006; 13:713–720

- S. G. Mougiakakou, I. K. Valavanis, A. Nikita, and K. S. Nikita, “Differential diagnosis of CT focal liver lesions using texture features, feature selection and ensemble driven classifiers,” Artif. Intell. Med. 41(1), 25–37 (2007).

- S. Gr. Mougiakakou1, I. Valavanis1, K. S. Nikita1, A. Nikita2, D. Kelekis2 Characterization of CT Liver Lesions Based on Texture Features and a Multiple Neural Network Classification Scheme , 2003 IEEE, pp.1287- 1291.

- S. S. Kumar, R. S. MONI. Diagnosis of Liver Tumor from CT Images using Curvelet Transform/ (IJCSE) International Journal on Computer Science and Engineering Vol. 02, No. 04, 2010, 1173-1178)

- R. M. Haralick, K. Shanmugam, and I. Dinstein, “Textural features for image classification," IEEE Transactions on In Systems, Man and Cybernetics, vol. 3, pp. 610-621, December 1973.

- Valavanis I, Mougiakakou SG, Nikita KS, Nikita A (2004) Computer Aided Diagnosis of CT Focal Liver Lesions by an Ensemble of Neural Network and Statistical Classifier. In: Proc. of International Conference of IEEE on Neural Networks 3:1929-1934

- Susan Standring , Gray's Anatomy, 40th Edition, The Anatomical Basis of Clinical Practice , May 2008 Elsevier Limited. All rights reserved , International Edition ISBN: 978-0-8089-2371-8

- Saladin • *Anatomy & Physiology: The Unity of Form and Function, Fifth Edition,* Copyright ©2009 by The McGraw−Hill Companies, Inc. All rights, http://www.primisonline.com ISBN−10: 0−39−099995−4 ISBN−13: 978−0−39−099995−5

- Yoshida, H.,D.Casalino, B. Keserci, A. Coskun, O. Ozturk and A. Savranlar (2003), *Waveletpacket- based texture analysis for differentiation between benign and malignant liver tumors in ultrasound images,* Physics in Medicine and Biology, No. 48, pp. 3735-375

- Shimizu A, Ito K, Koike S, Fujita T, Shimizu K, Matsunaga N. Cirrhosis or chronic hepatitis: evaluation of small (<or=2-cm) earlyenhancing hepatic lesions with serial contrast-enhanced dynamic MR imaging. Radiology 2003; 226:550-555.

- *Strunk H, Stuckmann G, Textor J, et al: Limitations and pitfalls of Couinaud's segmentation of the liver in transaxial imaging. Eur Radiol 13:2472-2482, 2003.)*

- Rutkauskas S, Gedrimas V, Pundzius J, et al: Clinical and anatomical basis for the classification of the structural parts of liver. Medicina (Kaunas) 42:98, 2006.